

Dear editor,

We wish to thank you, the two anonymous referees, and Dr H. Moosmüller for useful comments on the manuscript. We have carefully revised the text to improve the clarity of the reading.

In particular we have made a small change to the paper title from

“Spectral- and size-resolved mass absorption efficiency of mineral dust aerosols in the shortwave: a simulation chamber study”

to

“Spectral- and size-resolved mass absorption efficiency of mineral dust aerosols in the shortwave **spectrum**: a simulation chamber study”

The detailed answers to the two anonymous referees are presented

Anonymous Referee #1

The paper presents needed results on dust optical properties (mass absorption efficiency and absorption Angstrom exponent) for $D < 2.5 \mu\text{m}$ and $D < 10 \mu\text{m}$ particles, relating them to chemical composition. The samples analyzed are from 12 locations in northern Africa (5 samples), Namibia (1 sample), northern China (1 sample), the Middle East (2 samples), North America (1 sample), South America (1 sample) and Australia (1 sample). I have no substantial issues with the analysis or the paper. I recommend publication after addressing the minor points below:

1) In the Abstract and somewhere earlier in the paper (before the Results section) the location where the samples were collected from should be presented. Some information about sample collection is also needed – i.e.: a) Was only one sample collected at each location, or were multiple samples collected then combined? b) Were the samples collected from locations known to be preferential sources for atmospheric dust or was the collection location just random? The latter point is important, since it's known that atmospheric dust comes from preferential locations.

To address this point, the sentence in the result section has been rewritten as “The selection of these soils and sediments was made out of 137 individual top-soil samples collected in major arid and semi-arid regions worldwide and representing the mineralogical diversity of the soil composition at the global scale. As discussed in Di Biagio et al. (2017), this large sample set

was reduced by a set of 19 samples their availability in sufficient quantities for injection in the chamber. Because some of the experiments did not produce enough dust to perform good-quality optical measurements, , in this paper we present a set of twelve samples distributed worldwide but mostly in Northern and Western Africa (Libya, Algeria, Mali, Bodélé) and the Middle East (Saudi Arabia and Kuwait). Individual samples from the Gobi desert in Eastern Asia, the Namib Desert, the Strzelecki desert in Australia, the Patagonian deserts in South America, and the Sonoran Desert in Arizona have also been investigated.”

The first sentence of the abstract has been changed as ”This paper presents new laboratory measurements of the mass absorption efficiency (MAE) between 375 and 850 nm for twelve individual samples of mineral dust from different source areas worldwide and in two size classes”.

2) Abstract, pg. 2, lines 33-34: “The size-independence of AAE suggests that, for a given size distribution, the possible variation of dust composition with size would not affect significantly the spectral behavior of shortwave absorption.” Either that or the composition simply DIDN'T vary with size for this set of samples – so I'd reword this a bit.

This correction has been accepted

3) pg. 2, line 39: Need to spell out AAOD this first time that you use it.

This correction has been accepted

4) pg. 2, lines 40-41: “which is relevant to the development of remote sensing of light-absorption aerosols from space. ” Not only from space! This approach has also been used extensively for AERONET (surface-based remote sensing) AAOD attribution.

The reviewer is right, the sentence has been rewritten as “, which is relevant to the development of remote sensing of light-absorption aerosols from space, and their assimilation in climate models.”

5) pg. 3 line 56 contains a partial sentence (“In the solar spectrum (Boucher et al., 2013)”).

This was reworded as “Albeit partially compensated by the radiative effect in the thermal infrared, the global mean radiative effect of mineral dust in the shortwave is negative both at the surface and the top of the atmosphere (TOA) and local warming of the atmosphere (Boucher et al., 2013).”

6) pg. 6, lines 162-163: “The total uncertainty, including the effects of photon counting and the deposit inhomogeneity, on the absorption coefficient measurement is estimated at 8%.” Is there a basis/reference for this?

The references to the papers of Petzold et al. (2004) and Massabo' et al. (2013) have been added to the text.

7) pg. 7, line 170: It would be useful to give typical total masses and/or the fractional error/uncertainty in total aerosol gravimetric mass based on this error in filter mass.

This has been added in lines 173-175.

8) pg. 8, line 223 equation: When I read this my immediate question was: “How does this compare to the measure of total gravimetric mass?”. You answer this question (appropriately) in the results section but I still think it would be useful to add a note here pointing to the fact the in your results discussion you found this agreed well with the total gravimetric mass.

The following sentence has been added “As it will be explained in the result section (paragraph 3.1), the values of MCdust estimated from Equation 4 were found in excellent agreement with the measured gravimetric mass on the filters”

9) pg. 10: Do you have any estimate / sense of how well the dust suspended by this “shaking” compares to the dust lofted by winds?

Prior to any scientific analysis, we have dedicated a lot of energy to investigate the realism of our dust generation system, both in terms of the composition and the size distribution of the dust aerosols. These results are reported in two papers:

- Di Biagio, C., P. Formenti, S. A. Styler, E. Pangu, and J.-F. Doussin (2014), Laboratory chamber measurements of the longwave extinction spectra and complex refractive indices of African and Asian mineral dusts, *Geophys. Res. Lett.*, 41, doi:10.1002/2014GL060213. – Figure 2 and discussion

But in particular in

- Di Biagio, C., Formenti, P., Balkanski, Y., Caponi, L., Cazaunau, M., Pangu, E., Journet, E., Nowak, S., Caquineau, S., Andreae, M. O., Kandler, K., Saeed, T., Piketh, S., Seibert, D., Williams, E., and Doussin, J.-F.: Global scale variability of the mineral

dust long-wave refractive index: a new dataset of in situ measurements for climate modeling and remote sensing, *Atmos. Chem. Phys.*, 17, 1901-1929, doi:10.5194/acp-17-1901-2017, 2017

where we have dedicated two paragraphs (5.1. Atmospheric representativity: mineralogical composition and 5.2 Atmospheric representativity: size distribution) to show how the composition and the size distribution of the generated dust are well representative of those of real dust in the atmosphere, which makes the laboratory experiments well suited for studying the dust optical properties.

In order to stress this point further, without repeating results already presented in these two publications, we have added the following sentence in paragraph 3 “Di Biagio et al. (2014; 2017) have demonstrated the realism of the generation system concerning the composition and the size distribution of the generated dust with respect to the properties of mineral dust in the atmosphere”.

10) pg. 11, line 209: Mauritania is not listed as one of the sample site locations in Table 3. ?

For Mauritania, we only have chemical composition but not optical measurement results. The reference to this sample has been taken out of the paper.

11) pg. 11, lines 309-310 (an onward): The results here are said to agree well with that found for atmospheric aerosols in other studies, but the values in these studies is not given so this feels very hand-waving and unconvincing. Are you referring to the values given in Table 5? If so, please refer directly to them. If not, the comparison here needs to be more quantitative (discuss numbers from the literature vs. what is found here).

Additional text and values have been added in lines 321-392 to address this point

12) pg. 13, lines 353-354: If you have results for Niger why not show them?

We do not have optical results for Niger

13) pg. 14, lines 387-388: MAE doesn't vary linearly inversely with wavelength, it varies linearly inversely with the log of the wavelength (hence our ability to use the AAE relationship).

The reviewer is correct, this has been corrected as “and decrease in a linear way with the logarithm of the wavelength”

14) pg. 15, lines 429-434: A few things: a) “satisfactory” and “loose” are not quantitative terms, nor are they really appropriate for a scientific paper. What constitutes “satisfactory”? Best is to just give the correlations. b) The high correlation coefficients for PM_{2.5} are really driven by one high data point and so are probably not very robust.

These sentences have been reworded as “Regardless of the size fraction, the correlation between the MAE values and the percent mass of total elemental iron are higher at 375, 407 and 532 nm” and “At these wavelengths, linear correlations with the mass fraction of iron oxides are low in the PM_{10.6} mass fraction (R^2 up to 0.38-0.62), but higher in the PM_{2.5} fraction (R^2 up to 0.83-0.99)”

15) pg. 16, lines 455-456: How can fine-mode-only AOD be GREATER than total aerosol AOD?

Total and fine were inverted by mistake, this is now corrected

16) pg. 17, lines 487-488: As written this implies Solomon et al. varied SSA by 5%.

For, say, SSA of 0.9, that they varied SSA by 0.045. That is, the co-albedo (or absorption) was varied by 45% (0.1 ± 0.045). This is the proper comparison to make to the variation in MAE that you calculate

The reviewer is right. The sentence has been corrected as “As a comparison, Solmon et al. (2008) showed that varying the single scattering albedo of mineral dust over western Africa by $\pm 5\%$, that is, varying the co-albedo (or absorption) by 45% (0.1 ± 0.045) could drastically change the climate response in the region.”

7) Overall: Some editing is needed for language throughout. Here I list some that stood out to me – all small stuff but editing would help readability:

pg. 3, line 67-68: “in the last ten years or so” (too casual for scientific writing)

removed

pg. 3, line 74: “A significant body of observations have been performed.”

Replaced by “A significant number of observations have quantified”

pg. 8, lines 214-215: “The linear deconvolution, performed the Athena IFEFFIT free-ware analysis program (Ravel and Newville, 2005), provided with the proportionality factors α_i representing the mass fraction of elemental iron to be assigned to the i-th standard mineral.”
(I found this sentence nearly impossible to follow)

Replaced by “The linear deconvolution has been performed with the Athena IFEFFIT freeware analysis program (Ravel and Newville, 2005). This provided with the proportionality factors α_i representing the mass fraction of elemental iron to be assigned to the i-th standard mineral.”

pg. 10, line 253: “the chamber was evacuated by to” (delete “by”)

Corrected

pg. 10, line 259: “dust particles produced was” → “dust particles produced were”

The sentence was corrected as “The dust particles produced by the mechanical shaking, mimicking the saltation processing that soils experience when eroded by strong winds, were injected in the chamber by flushing the flask with N₂ at 10 L min⁻¹ for about 10-15 min, whilst continuing shaking the soil.”

pg. 10, lines 279 “dust on filter for” → “dust on the filter for”

Corrected as “dust on the filter membranes for subsequent chemical analysis”

pg. 10, line 280: “by placing the loaded filter holders”: This reads as if you are placing LOADED FILTERS (vs holders with blank filters in them, which is what I assume you mean). Reword.

Corrected as “by placing the filter holders loaded with filter membranes”

pg. 11, line 206: “the origin of used dust samples”. I think this should be “the origin of our dust samples”, yes?

Corrected as “the origin of dust samples”

pg. 12, line 315: “Henceforth, and contrary to the soil samples”

pg. 12, lines 317-318: “could reflect more that of the parent sedimentary soil than not the other samples.”

These two sentences were rewritten as “This powder is likely to be injected in the chamber with little or no size fractionation. Henceforth, the aerosol generated from it should have a closer composition to the original powder than the other samples.

pg. 12, line 335: “An the exception”

Corrected as “Exceptions are”

pg. 13, lines 353-354: “As a matter of fact, the number fraction of particles in the size classes above 0.5 μm in diameter are different in the dust aerosol generated in the Alfaro et al. (2004) study with respect to ours.”

Corrected as “As a matter of fact, the number fraction of particles in the size classes above 0.5 μm in diameter is different in the dust aerosol generated in the Alfaro et al. (2004) study with respect to ours.”

pg. 13, line 364: “On the contrary” \rightarrow “In contrast

Corrected

pg. 13, line 365: “These differences could yield either to difference in the”

Corrected as “These differences could either be due to difference in the chemical composition and/or in the total mass in the denominator of Equation 8.”

pg. 15, lines 415-417: “using a power-law function fit as from Equation 2, provides withthe values of”

Corrected as “using the power-law function fit (Equation 2)”

pg. 16, line 448: “The size-dependence, yielding significantly higher MAE values”

Corrected as “The size-dependence, yielding significantly higher MAE values in the fine fraction (PM_{2.5}) than in the bulk (PM_{10.6}) aerosol,”

pg. 17, line 470: “A closer look to observations” → “A closer look at observations”

Corrected as “These differences could either be due to difference in the chemical composition and/or in the total mass in the denominator of Equation 8.”

pg. 17, line 478: “our estimated MAE average at” → “our average MAE values are”

Corrected

pg. 17, line 490: “As Moosmuller et al.” → “As in Moosmuller et al.”

Corrected

pg. 18, line 503-504: “pointing out to the” → “pointing out the

Corrected

Anonymous Referee #2

GENERAL COMMENT

The manuscript presents important results from a carefully designed and conducted study on the light-absorbing properties of mineral dust from various origins. Dust samples collected at the different source regions have been re-suspended in an aerosol chamber and characterized with respect to microphysical, optical and chemical properties by state of the art methods. The study provides urgently needed knowledge on the multi-spectral light absorbing properties of mineral dust and for sure deserves publication in ACP. The manuscript is well structured, the methods are described in necessary detail and the referenced literature reflects the current state of knowledge. I recommend publication after the following minor revisions have been considered.

SPECIFIC REMARKS

1. In the experimental protocol section, the potential impact of gravitational settling on the re-suspended fraction of the dust samples is mentioned.

Given the instrumentation list, the size distributions of the airborne dust samples were monitored during the runs of the experiments. It appears obvious to control the change of the size distribution during the experiment time in the chamber. Since the mass concentration in the chamber decreased very rapidly after injection, whereas the chemical composition of the dust samples was determined from bulk samples, it would be important to know if the airborne fraction sampled for the determination of optical properties features the same chemical properties as the bulk samples. At least a discussion of this potential source of uncertainties should be presented, along with a plot showing the change of the size distributions during the experiment time. The current analysis starts from the assumption that the dust bulk properties represent also the properties of the sampled airborne fractions. However, is this really justified?

The reviewer is right when saying that the samples collected for the investigation of the chemical composition are time-integrated and henceforth might reproduce dust with varying size distributions. Examples of the time variability of the size distributions are provided by Di Biagio et al. (2017) - Figures 7 and 5S in the supplementary material. These figures show that, after the very strong initial depletion of particles larger than 10 μm in diameter (when no sampling on filters was performed), the number concentration decreases at a rate, which is almost independent of size, suggesting that no significant distortion of the particle size distribution occurs after the most significant removal at the beginning of the experiment.

We also would like to stress that our generation system allows to generate a dust aerosol from a soil, and that this dust aerosol is injected in the chamber, not the soil. Henceforth, when talking about "bulk" we refer to the total aerosol fraction, sampled from the chamber without any size segregation other than that imposed by the cutoff the sampling lines. The fine fraction corresponds to the same dust aerosols, but sampled by an impactor with a 2.5 diameter cutoff.

2. In section 3.2, the variability of dust optical properties with particle size is discussed. The authors found no statistically significant size-dependence of the absorption Ångström exponent (AAE), whereas the absolute values of the mass absorption efficiencies (MAE) show large differences between the PM_{2.5} and PM₁₀ fractions with larger values for the fine mode fraction.

These findings imply that the relative chemical composition with respect to light-absorbing compounds does not change between the size fractions (similar AAE values), whereas the differences between the MAC values indicate that coarse mode particles contain more non-absorbing matter than fine mode particles (higher MAE values for smaller particles). This however, this is in contrast to the assumption that the chemical composition is uniformly distributed across the particle size distribution. Here, a detailed discussion is requested.

The reviewer's statement is in error as for a given mineral composition (given effective complex refractive index) the MAE depends strongly on size, decreasing with size at larger sizes. So having a smaller MAE for PM₁₀ than for PM_{2.5}, does not necessarily imply that PM₁₀ contains less absorbing matter than PM_{2.5}, but may just be due to the change in size distribution. This is shown by our calculations. An independent example of the size dependence is also given by Fig. 1 of Moosmüller et al. (2009).

Moosmüller, H., R. K. Chakrabarty, and W. P. Arnott (2009), Aerosol light absorption and its measurement: A review, *Journal of Quantitative Spectroscopy and Radiative Transfer*, 110(11), 844-878.

3. In section 4, it is discussed that the potential impact of light absorption by mineral dust may play an important role even after long range transport. Cited studies all refer to observations in China.

However, there is another detailed study on this effect available for the pollution plume of Dakar mixing with mineral dust which also includes the variation of the AAE during mixing (Petzold et al., 2011). The authors may consider including this study.

This reference has been added to the manuscript.

MINOR COMMENTS

1. The list of references contains various references which are not cited in the manuscript. This should be checked, I found the following but there may be more: Anderson et al., 1998, Andrews et al., 2006, Arnott et al., 2005, Collaud Coen et al., 2010, Petzold et al., 2013.

Corrected

2. Line 56: The sentence seems to be incomplete.

The sentence was corrected as “Albeit partially compensated by the radiative effect in the thermal infrared, the global mean radiative effect of mineral dust in the shortwave is negative both at the surface and the top of the atmosphere (TOA) and local warming of the atmosphere (Boucher et al., 2013).”

3. Line 97 – 98: The basic unit of mass concentrations is gm^{-3} . Using this unit, then the unit of the combined property MAE is $\text{m}^2 \text{g}^{-1}$ as stated. In its current version this link is not clearly visible.

4. Line 102: The sentence seems to be incomplete.

The sentence was removed

5. Line 163: A reference for the uncertainty of the MWAA is required.

This has been added

6. Line 912: Please check for correct reference, there is no reference Petzold et al. (2008) in the list of references.

Corrected

7. In Figure 4, regression lines may be shown as full line to improve their visibility.

Done

TYPOS

1. Line 108: It should read: “absorption Ångström exponent”.

Corrected

2. Line 138: Skip “with”.

Corrected

3. Line 165: It should read “deposited on a filter ...”.

Corrected

4. Line 245: It should read: “the uncertainty of values ...”.

Corrected

5. Line 253: Skip “by”.

Corrected

6. Line 338: It should read: “PM2.5 fraction”.

Corrected

7. Line 426 –427: I assume the Figures 4 are referenced here.

Corrected

REFERENCES

Petzold, A., Veira, A., Mund, S., Esselborn, M., Kiemle, C., Weinzierl, B., Hamburger, T., Ehret, G., Lieke, K., and Kandler, K.: Mixing of mineral dust with urban pollution aerosol over Dakar (Senegal): impact on dust physico-chemical and radiative properties, *Tellus*, 63B, 619-634, doi: 10.1111/j.1600-0889.2011.00547.x, 2011.

1 **Spectral- and size-resolved mass absorption efficiency of mineral dust aerosols in**
2 **the shortwave spectrum: a simulation chamber study**

3 Lorenzo Caponi^{1,2}, Paola Formenti¹, Dario Massabó², Claudia Di Biagio¹, Mathieu Cazaunau¹, Edou-
4 ard Pangui¹, Servanne Chevaillier¹, Gautier Landrot³, Meinrat O. Andreae^{4,11}, Konrad Kandler⁵, Stuart
5 Piketh⁶, Thuraya Saeed⁷, Dave Seibert⁸, Earle Williams⁹, Yves Balkanski¹⁰, Paolo Prati², and Jean-
6 François Doussin¹

7 ¹ *Laboratoire Interuniversitaire des Systèmes Atmosphériques (LISA), UMR 7583, CNRS, Université Paris-Est-*
8 *Créteil et Université Paris Diderot, Institut Pierre Simon Laplace, Créteil, France*

9 ² *University of Genoa, Department of Physics & INFN, Genoa, Italy*

10 ³ *Synchrotron SOLEIL, L'Orme des Merisiers Saint-Aubin, France*

11 ⁴ *Biogeochemistry Department, Max Planck Institute for Chemistry, P.O. Box 3060, 55020, Mainz, Germany*

12 ⁵ *Institut für Angewandte Geowissenschaften, Technische Universität Darmstadt, Schnittspahnstr. 9, 64287*
13 *Darmstadt, Germany*

14 ⁶ *Climatology Research Group, University of the Witwatersrand, Johannesburg, South Africa*

15 ⁷ *Science Department, College of Basic Education, Public Authority for Applied Education and Training, Al-*
16 *Ardeya, Kuwait*

17 ⁸ *Walden University, Minneapolis, Minnesota, USA*

18 ⁹ *Massachusetts Institute of Technology, Cambridge, Massachusetts, USA*

19 ¹⁰ *LSCE, CNRS UMR 8212, CEA, Université de Versailles Saint-Quentin, Gif sur Yvette, France*

20 ¹¹ *Geology and Geophysics Department, King Saud University, Riyadh, Saudi Arabia*

21
22 * Corresponding author: paola.formenti@lisa.u-pec.fr
23

24 Abstract

25 This paper presents new laboratory measurements of the mass absorption efficiency (MAE) between
26 375 and 850 nm for [twelve individual samples of](#) mineral dust [from different source areas worldwide](#)
27 [and in of different origin](#) in two size classes: PM_{10.6} (mass fraction of particles of aerodynamic diameter
28 lower than 10.6 μm) and PM_{2.5} (mass fraction of particles of aerodynamic diameter lower than 2.5 μm).
29 ~~The~~ experiments ~~have been~~ were performed in the CESAM simulation chamber using ~~generated~~-min-
30 eral dust generated from natural parent soils, and included optical and gravimetric analyses.

31 ~~The R~~results show that the MAE values are lower for the PM_{10.6} mass fraction (range 37-135 10⁻³ m² g⁻¹
32 at 375 nm) than for the PM_{2.5} (range 95-711 10⁻³ m² g⁻¹ at 375 nm), and decrease with increasing wave-
33 length as λ^{-AAE} , where the Angstrom Absorption Exponent (AAE) averages between 3.3-3.5, regardless
34 of size. The size-independence of AAE suggests that, for a given size distribution, the ~~possible variation~~
35 ~~of dust composition~~ did not vary with size for this set of samples~~with size would not affect significantly~~
36 ~~the spectral behavior of shortwave absorption~~. Because of its high atmospheric concentration, light-
37 absorption by mineral dust can be competitive ~~to~~ with black and brown carbon even during atmospheric
38 transport over heavy polluted regions, when dust concentrations are significantly lower than at emission.
39 The AAE values of mineral dust are higher than for black carbon (~1), but in the same range as light-
40 absorbing organic (brown) carbon. As a result, depending on the environment, there can be some ambi-
41 guity in apportioning the aerosol absorption optical depth (AAOD) based on spectral dependence, which
42 is relevant to the development of remote sensing of light-absorbing aerosols ~~from space~~, and their
43 assimilation in climate models. We suggest that the sample-to-sample variability in our dataset of MAE
44 values is related to regional differences ~~of~~ in the mineralogical composition of the parent soils. Particu-
45 larly in the PM_{2.5} fraction, we found a strong linear correlation between the dust light-absorption prop-
46 erties and elemental iron rather than the iron oxide fraction, which could ease the application and the
47 validation of climate models that now start to include the representation of the dust composition, as well
48 as for remote sensing of dust absorption in the UV-VIS spectral region.

49 1. Introduction

50 Mineral dust aerosols emitted by wind erosion of arid and semi-arid soils account for about 40% of the
51 total emitted aerosol mass per year at the global scale (Knippertz and Stuut, 2014). The episodic but
52 frequent transport of intense mineral dust plumes is visible from spaceborne sensors, as their high con-
53 centrations, combined with ~~to~~ their ability of ~~to~~ scattering and absorbing solar and thermal radiation,

54 give raise to the highest registered values of aerosol optical depth (AOD) on Earth (Chiapello, 2014).
55 The instantaneous radiative efficiency of dust particles, that is, their radiative effect per unit AOD, is of
56 the order of tenths to hundreds of $W m^{-2} AOD^{-1}$ in the solar spectrum, and of the order of order of tenths
57 of $W m^{-2} AOD^{-1}$ in the thermal infrared (e.g., Haywood et al., 2003; di Sarra et al., 2011; Slingo et al.,
58 2006 and the compilation of Highwood and Ryder, 2014). ~~In the solar spectrum, (Boucher et al., 2013).~~
59 Albeit partially compensated by the radiative effect in the thermal infrared, the global mean radiative
60 effect of mineral dust in the shortwave is negative both at the surface and the top of the atmosphere
61 (TOA) and produces a local warming of the atmosphere (Boucher et al., 2013). ~~Many-There are the~~
62 ~~consequences-numerous impacts of dust on the~~ global and regional climate, ~~that-which~~ ultimately feed
63 back on wind speed and vegetation and therefore on dust emission (Tegen and Lacis, 1996; Solmon et
64 al., 2008; Pérez et al., 2006; Miller et al., 2014). Dust particles perturb the surface air temperature
65 through their radiative effect at TOA, can increase the atmospheric stability (e.g., Zhao et al. 2011) and
66 might affect precipitation at the global and regional scale (Solmon et al., 2008; Xian, 2008; Vinoj et al.,
67 2014; Miller et al., 2014 and references therein).

68 All models ~~show-indicate~~ that the effect of mineral dust on climate has a great sensitivity to their
69 shortwave absorption properties ~~of mineral dust~~ (Miller et al., 2004; Lau et al., 2009; Loeb and Su, 2010;
70 Ming et al., 2010; Perlwitz and Miller, 2010). Absorption by mineral dust started receiving a great deal
71 of interest ~~in the last ten years or so~~, when spaceborne and ground-based remote sensing studies (Dubovik
72 et al., 2002; Colarco et al., 2002; Sinyuk et al., 2003) suggested that mineral dust was less absorbing
73 ~~that-thani~~ had been ~~suggested indicated~~ by in situ observations (e.g., Patterson et al., 1977; Haywood et
74 al., 2001), particularly at wavelengths below 600 nm. Balkanski et al. (2007) showed that lowering the
75 dust absorption properties to an extent that reconciles them both with the remote-sensing observations
76 and the state-of-knowledge of the mineralogical composition, allowed calculating ~~the~~ clear-sky ~~dust~~
77 shortwave radiative effect ~~of dust~~ in agreement with satellite-based observations. A significant ~~body~~
78 ~~number~~ of observations has ~~ve-been-performed-in-quantify-quantifieding~~ the shortwave light-absorbing
79 properties of mineral dust, by direct measurements (Alfaro et al., 2004; Linke et al., 2006; Osborne et
80 al., 2008; McConnell et al., 2008; Derimian et al., 2008; Yang et al., 2009; Müller et al., 2009; Petzold
81 et al., 2009; Formenti et al., 2011; Moosmüller et al., 2012; Wagner et al., 2012; Ryder al., 2013a; Utry
82 et al., 2015; Denjean et al., 2015c; 2016), and indirectly, by quantifying the amount and the speciation
83 of the light-absorbing compounds in mineral dust, principally iron oxides (Lafon et al., 2004; 2006;

84 Lazaro et al., 2008; Derimian et al., 2008; Zhang et al., 2008; Kandler et al., 2007; 2009; 2011; Formenti
85 et al., 2014a; 2014b).

86 However, existing data are often limited to a single wavelength, which moreover ~~are-is~~ not the same
87 identical for all experiments. Also, frequently they do not represent the possible regional variability of
88 the dust absorption, either because they are obtained from field measurements integrating the contribu-
89 tions of different source regions, or conversely, by laboratory investigations targeting samples from a
90 limited number of locations. This might lead to biases in the data. Indeed, iron oxides in mineral dust,
91 mostly in the form of hematite (Fe₂O₃) and goethite (Fe(O)OH), have specific absorption bands in the
92 UV-VIS spectrum (Bédidi and Cervelle, 1993), and have a variable content depending on the soil min-
93 eralogy of the source regions (Journet et al., 2014).

94 ~~Henceforth, i~~In this study, ~~e~~Experiments on twelve aerosol samples generated from natural parent top
95 soils from various source regions worldwide have been ~~were~~ conducted with a large atmospheric simu-
96 lation chamber. ~~we~~We present a new evaluation of the ultraviolet to near-infrared (375-850 nm) light-
97 absorbing properties of mineral dust by ~~studying-investigating~~ the size-segregated mass absorption effi-
98 ciency (MAE, units of m² g⁻¹) and its spectral dependence, ~~largely-widely~~ used in climate models to
99 calculate the direct radiative effect of aerosols. ~~Experiments on twelve aerosol samples generated from~~
100 ~~natural parent top soils from various source regions worldwide have been conducted with a large atmos-~~
101 ~~pheric simulation chamber.~~

102 2. Instruments and methods

103 At a given wavelength, λ , the mass absorption efficiency (MAE, units of m² g⁻¹) is defined as the ratio
104 of the aerosol light-absorption coefficient $b_{\text{abs}}(\lambda)$ (units of m⁻¹), and its mass concentration (in $\mu\text{g m}^{-3}$)

105

$$106 \quad MAE(\lambda) = \frac{b_{\text{abs}}(\lambda)}{\text{Mass Conc}} \quad (1)$$

107

108 ~~MAE values for mineral dust aerosol are expressed in~~ MAE values for mineral dust aerosol are ex-
109 pressed in 10⁻³ m² g⁻¹.

110 The spectral dependence of the aerosol absorption coefficient $b_{\text{abs}}(\lambda)$ is described by the power-law
111 relationship

112

113

$$b_{abs}(\lambda) \sim \lambda^{-AAE} \quad (2)$$

114

115 where the AAE is the [Absorption Ångström Absorption](#)-Exponent, representing the negative slope of
116 $b_{abs}(\lambda)$ in a log-log plot (Moosmüller et al., 2009)

117

$$AAE = -\frac{d\ln(b_{abs}(\lambda))}{d\ln(\lambda)} \quad (3)$$

118

120 **2.1. The CESAM simulation chamber**

121 [The e](#)Experiments in this work have been performed in the 4.2 m³ stainless-steel CESAM (French acro-
122 nym for Experimental Multiphasic Atmospheric Simulation Chamber) simulation chamber (Wang et al.,
123 2011). The CESAM chamber has been extensively used in recent years to simulate, at sub and super-
124 saturated conditions, the formation and properties of aerosols at concentration levels comparable to those
125 encountered in the atmosphere (Denjean et al., 2015a; 2015b; [Brégonzio-Rozier et al., 2015; 2016; Di](#)
126 [Biagio et al., 2014; 2017](#)).

127 CESAM is a multi-instrumented platform, equipped with twelve circular flanges to support its analytical
128 environment. Basic instrumentation comprises sensors to measure the temperature, pressure and relative
129 humidity within the chamber (two manometers MKS Baratron (MKS, 622A and MKS, 626A) and a
130 HMP234 Vaisala® humidity and temperature sensor). The particle size distribution is routinely meas-
131 ured by a combination of (i) a scanning mobility particle sizer (SMPS, mobility diameter range 0.02–
132 0.88 µm), composed of a Differential Mobility Analyzer (DMA, TSI Inc. Model 3080) and a Condensa-
133 tion Particle Counter (CPC, TSI Inc. Model 3772); (ii) a SkyGrimm optical particle counter (Grimm
134 Inc., model 1.129, optical equivalent diameter range 0.25–32 µm); and (iii) a WELAS optical particle
135 counter (PALAS, model 2000, optical equivalent diameter range 0.5–47 µm). Full details of operations
136 and data treatment of the particle counters are provided in [Di Biagio et al. \(2016, 2017\)](#).

137 **2.2. Filter sampling**

138 Three filter samples per top soil sample were collected on different types of substrate based on the anal-
139 ysis to [be performed](#). Sampling dedicated to the determination of the aerosol mass concentration by

140 gravimetric analysis and the measurement of the absorption coefficients by optical analysis was per-
141 formed on 47-mm quartz membranes (Pall Tissuquartz™, 2500 QAT-UP). Two samples were collected
142 in parallel. The first quartz membrane sample (“total”) was collected without a dedicated size cut-off
143 using an in-house built stainless steel sampler operated at 5 L min⁻¹. However, as detailed in Di Biagio
144 et al. (2016, 2017), the length of the sampling line from the intake point in the chamber to the filter en-
145 trance was 50 cm, yielding resulting in with a 50% cut-off of the transmission efficiency at 10.6 μm in
146 particle aerodynamic diameter. This fraction is therefore indicated as PM_{10.6} in the forthcoming follow-
147 ing discussion. The second quartz membrane sample was collected using a 4-stage DEKATI impactor
148 operated at the a flow rate of 10 L min⁻¹ to select the aerosol fraction of particles with aerodynamic
149 diameter smaller than 2.5 μm, indicated as PM_{2.5} here forth. Sampling for the analysis of the iron oxide
150 content was performed on polycarbonate filters (47-mm Nuclepore, Whatman; pore size of 0.4 μm)
151 using the same sample holder than as used for the total quartz filters, and therefore referring correspond-
152 ing to the PM_{10.6} mass fraction. Samples were collected at a flow rate of 6 L min⁻¹. All flow rates were
153 monitored by a thermal mass flow meter (TSI Inc., model 4140). These samples were also used to de-
154 termine the elemental composition (including Fe) and the fraction of iron oxides in the total mass.

155 2.3. The Multi-Wavelength Absorbance Analyzer (MWAA)

156 The aerosol absorption coefficient, $b_{\text{abs}}(\lambda)$, at 5 wavelengths ($\lambda = 375, 407, 532, 635$, and 850 nm) was
157 measured by *in situ* analysis of the quartz filter samples using the Multi-Wavelength Absorbance Ana-
158 lyzer (MWAA), described in detail in Massabò et al. (2013; 2015).

159 The MWAA performs a non-destructive scan of the quartz filters on at 64 different points, each ~ 1 mm²
160 wide. It measures the light transmission through the filter as well as backscattering at two different angles
161 (125° and 165°). This is necessary to constrain the multiple scattering effects occurring within the par-
162 ticle-filter system. The measurements are used as input of to a radiative transfer model (Hänel, 1987;
163 1994) as implemented by Petzold and Schönlinner (2004) for the Multi-Angle Absorption Photometry
164 (MAAP) measurements. In this model, a two stream approximation is applied (Coakley and Chylek,
165 1975), in which the fractions of hemispherical backscattered radiation with respect to the total scattering
166 for collimated and diffuse incident radiation are approximated on the basis of the Henyey-Greenstein
167 scattering phase function (Hänel, 1987). This approximation assumes a wavelength-independent asym-
168 metry parameter (g) set to 0.75, appropriate for mineral dust (Formenti et al., 2011; Ryder et al., 2013b).

169 The total uncertainty, including the effects of photon counting and the deposit inhomogeneity, on the
170 absorption coefficient measurement is estimated at 8% [\(Massabò et al., 2013\)](#).

171 **2.4. Gravimetric analysis**

172 The aerosol mass deposited on [the filters](#) (μg) was obtained by weighing the quartz filter before and after
173 sampling, after a period of 48 hours of conditioning in a room with controlled atmospheric conditions
174 (temperature, $T \sim 20 \pm 1 \text{ }^\circ\text{C}$; relative humidity, $\text{RH} \sim 50 \pm 5\%$). Weighing is performed with an analyt-
175 ical balance (Sartorius model MC5, precision of $1 \mu\text{g}$), and repeated three times to control the statistical
176 variability of the measurement. Electrostatic effects are removed by exposing the filters, prior weighing,
177 to a de-ionizer. The error ~~on~~[in](#) the measured mass is estimated at $1\theta \mu\text{g}$, including the repetition varia-
178 bility. The aerosol mass concentration ($\mu\text{g m}^{-3}$) is obtained by dividing the mass deposited on [the filter](#)
179 to the total volume of sampled air (m^3) obtained from the mass flowmeter measurements [\(+5%\)](#). [The](#)
180 [percent error on mass concentrations is estimated to 5%](#).

181 **2.5. Dust composition measurements**

182 **2.5.1. Elemental composition**

183 Elemental concentrations for the major constituents of mineral dust (Na, Mg, Al, Si, P, S, Cl, K, Ca, Fe,
184 Ti, Mn) were obtained by ~~a~~-Wavelength Dispersive X-ray ~~fluorescence~~[Fluorescence](#) (WD-XRF) of the
185 Nuclepore filters using a PW-2404 spectrometer by Panalytical. Excitation X-rays are produced by a
186 Coolidge tube ($I_{\text{max}} = 125 \text{ mA}$, $V_{\text{max}} = 60 \text{ kV}$) with a Rh anode; [the](#) primary X-ray spectrum can be
187 controlled by inserting filters (Al, at different thickness) between the anode and the sample. Each ele-
188 ment was analyzed three times, with specific conditions (voltage, tube filter, collimator, analyzing crys-
189 tal, and detector). Data collection was controlled by the SuperQ software provided with the instrument.
190 The elemental mass thickness ($\mu\text{g cm}^{-2}$), that is, the analyzed elemental mass per unit surface, was ob-
191 tained by comparing the elemental yields with a sensitivity curve measured in the same geometry on a
192 set of certified mono- or bi-elemental thin layer standards by Micromatter Inc. The certified uncertainty
193 [of](#) the standard deposit ($\pm 5\%$) determines the lower limit [of](#) the uncertainty [of](#) the measured ele-
194 mental concentrations, which ranges between 8% and 10% depending on the [element](#) considered-~~ele-~~
195 [ment](#). Thanks to the uniformity of the aerosol deposit on the filters, the atmospheric elemental concen-
196 trations ($\mu\text{g m}^{-3}$) were calculated by multiplying the analyzed elemental mass thickness by the ratio
197 between the collection and analyzed surfaces of each sample (41 and 22 mm, respectively), then di-
198 [viding](#) by the total sampled volume (m^3). Finally, concentrations of light-weight elements (atomic

199 number $Z < 19$) were corrected for the underestimation induced by the self-absorption of the emitted
200 soft X-rays inside aerosol particles according to Formenti et al. (~~2014~~2010).

201 Additional XRF analysis of the quartz filters ~~was has been~~ performed both in the PM_{10.6} and the PM_{2.5}
202 fractions, ~~so~~ to verify the absence of biases between the experiments dedicated to the determination of
203 particle composition ~~to and~~ those where the optical properties were measured.

204 **2.6.2. Iron oxide content**

205 The content and the mineralogical speciation of the iron oxides, also defined as free-iron, ~~that is i.e.~~, the
206 fraction of iron ~~which that~~ is not in the crystal lattice of silicates (Karickhoff and Bailey, 1973), was
207 determined by XANES (X-ray absorption near-edge structure) in the Fe K-range (K_{α} , 7112 eV) at the
208 SAMBA (Spectroscopies Applied to Materials based on Absorption) beamline at the SOLEIL synchro-
209 tron facility in Saclay, France (Briois et al., 2011). The position and shape of the K pre-edge and edge
210 peaks were analyzed as they depend on the oxidation state of iron and the atomic positions of the neigh-
211 boring ions, mostly O^+ and OH^- .

212 As in Formenti et al. (2014b), samples were mounted in an external setup mode. A Si(220) double-
213 crystal monochromator was used to produce a monochromatic X-ray beam, which was $3000 \times 250 \mu m^2$
214 in size at the focal point. The energy range was scanned from 6850 eV to 7800 eV at a step resolution
215 varying between 0.2 eV in proximity to the Fe-K absorption edge (at 7112 eV) to 2 eV in the extended
216 range. Samples were analyzed in fluorescence mode without prior preparation. One scan acquisition
217 lasted approximately 30 minutes, and was repeated three times to improve the signal-to-noise ratio.

218 The same analytical protocol was applied to five standards of Fe(III)-bearing minerals (**Table 1**), includ-
219 ing iron oxides (hematite, goethite) and silicates (illite, montmorillonite, nontronite). The standard spec-
220 tra were used to deconvolute the dust sample spectra to quantify the mineralogical status of iron. The
221 linear deconvolution ~~was~~, performed with the Athena IFEFFIT freeware analysis program (Ravel and
222 Newville, 2005). ~~This~~, provided ~~with~~ the proportionality factors, α_{i-} , representing the mass fraction of
223 elemental iron to be assigned to the i -th standard mineral. In particular, the values of α_{hem} and α_{goe}
224 represent the mass fractions of elemental iron that can be attributed to hematite and goethite, and $\alpha_{Fe\ ox}$
225 ($\alpha_{hem} + \alpha_{goe}$), the mass fraction of elemental iron that can be attributed to iron oxides.

226 **2.6.3. Calculation of the iron oxide content**

227 The measured elemental concentrations obtained by X-ray Fluorescence (XRF) are expressed in the
 228 form of elemental oxides and summed to estimate the total mineral dust mass concentration MC_{dust} ac-
 229 cording to the equation from Lide (1992)

230

$$231 \quad [MC_{dust}] = 1.12 \times \left\{ \begin{array}{l} 1.658[Mg] + 1.889[Al] + 2.139[Si] + 1.399[Ca] + 1.668[Ti] + 1.582[Mn] \\ + (0.5 \times 1.286 + 0.5 \times 1.429 + 0.47 \times 1.204)[Fe] \end{array} \right\} \quad (4)$$

232

233 The relative uncertainty ~~on~~ in MC_{dust} , estimated from the analytical error ~~in~~ the measured
 234 concentrations, does not exceed 6%. [As it will be explained in the result section \(paragraph 3.1\), the](#)
 235 [values of \$MC_{dust}\$ estimated from Equation 4 were found in excellent agreement with the measured](#)
 236 [gravimetric mass on the filters.](#)

237 The fractional mass ratio (in percent) of elemental iron ($MR_{Fe\%}$) with respect to the total dust mass con-
 238 centration, MC_{dust} , is then calculated as

239

$$240 \quad MR_{Fe\%} = \frac{[Fe]}{[MC_{Dust}]} \times 100 \quad (5)$$

241

242 The mass concentration of iron oxides or free-iron ($MC_{Fe\ ox}$), representing the fraction of elemental iron
 243 in the form of hematite and goethite (Fe_2O_3 and $FeOOH$, respectively), is equal to

244

$$245 \quad MC_{Fe\ ox} = MC_{hem} + MC_{goe} \quad (6)$$

246

247 where MC_{hem} and MC_{goe} are the total masses of hematite and goethite. These can be calculated from the
 248 values α_{hem} and α_{goe} from XANES analysis, which represent the mass fractions of elemental iron at-
 249 tributed to hematite and goethite, as

250

$$251 \quad MC_{hem} = \frac{\alpha_{hem} \times [Fe]}{0.70} \quad (7.a)$$

$$MC_{goe} = \frac{\alpha_{goe} \times [Fe]}{0.63} \quad (7.b)$$

where the values of 0.70 and 0.63 represent the mass molar fractions of Fe in hematite and goethite, respectively. The relative errors of MC_{hem} and MC_{goe} are obtained from the uncertainties of the values of α_{hem} and α_{goe} from XANES analysis (less than 10%).

The mass ratio of iron oxides ($MR_{Fe\ ox\%}$) with respect to the total dust mass can then be calculated as

$$MR_{Fe\ ox\%} = MC_{Fe\ ox} \times MR_{Fe\ \%} \quad (8)$$

3. Experimental protocol

At the beginning of each experiment, the chamber was evacuated by to 10^{-4} - 10^{-5} hPa. Then, the reactor was filled with a mixture of 80% N₂ and 20% O₂ at a pressure slightly exceeding the current atmospheric pressure, in order to avoid contamination from ambient air. The experiments were conducted at ambient temperature and at a relative humidity <2%. As in Di Biagio et al. (2014; 2016,2017), dust aerosols were generated by mechanical shaking of the parent soils, previously sieved to < 1000 μ m and dried at 100 °C for about 1 h to remove any residual humidity. About 15 g of soil was placed in a Buchner flask and shaken for about 30 min at 100 Hz by means of a sieve shaker (Retsch AS200). The dust particles produced by the mechanical shaking, mimicking the saltation processing that soils experience when eroded by strong winds, as were then injected in the chamber by flushing the flask with N₂ at 10 L min⁻¹ for about 10-15 min, whilst continuing shaking the soil. Di Biagio et al. (2014; 2017) have demonstrated the realism of the generation system concerning the composition and the size distribution of the generated dust with respect to the properties of mineral dust in the atmosphere.

The dust was injected for about 10-15 minutes, and left remained suspended in the chamber for approximately 120 min thanks to the 4-wheel fan located in the bottom of the chamber body. Previous measurements at the top and bottom of the chamber showed that the fan ensures a homogeneous distribution of the dust starting approximately 10 minutes after the end of the injection (Di Biagio et al., 2014).

279 To compensate for the air extracted from the chamber by sampling, a particle-free flow of N₂/O₂, regu-
280 lated in real time as a function of the total volume of sampled air, was re-injected in the chamber. To
281 avoid excessive dilution the flow was limited to 20 L min⁻¹. Two experiments per soil type were con-
282 ducted: a first experiment for sampling on the nuclepore polycarbonate filters (determination of the ele-
283 mental composition and the iron oxide fraction) and *in situ* measurements of the infrared optical con-
284 stants (Di Biagio et al., 20162017), and a second experiment [sampling](#) on total quartz filter and impactor
285 for the study of dust MAE presented in this paper.

286 **Figure 1** illustrates as typical example the time series of the aerosol mass concentration during the two
287 experiments conducted for the Libyan sample. The comparison demonstrates the repeatability of the dust
288 concentrations, both in absolute values and in temporal dynamics. It also shows that the mass concen-
289 trations decreased very rapidly by gravitational settling within the first 30 minutes of the experiment
290 (see also the discussion in Di Biagio et al., (20162017)), after which concentrations only decrease by
291 dilution. The filter sampling was started after this transient phase, and then continued through the end of
292 the experiments, in order to collect enough dust on [the filter membranes](#) for [subsequent the](#) chemical
293 analysis. Blank samples were collected before the start of the experiments by placing the [loaded filter](#)
294 holders [loaded with filter membranes](#) in line with the chamber and by flushing them for a few seconds
295 with air coming from the chamber.

296 At the end of each experimental series with a given soil sample, the chamber was manually cleaned in
297 order to remove carry-over caused by resuspension of particles deposited to the walls. Background con-
298 centrations of aerosols in the chamber vary between 0.5 and 2.0 µg m⁻³, i.e., a factor of 500 to 1000
299 below the operating conditions.

300 **34. Results and discussion**

301 The geographical location of the soil collection sites is shown in **Figure 2**, [whereas-and](#) the coordinates
302 are summarized in **Table 2**. [As-discussed-in-Di-Biagio-et-al.\(2016\),the-selection-of-these-soils-and](#)
303 [sediments-was-governed-by-the-need-of-representing-the-major-arid-and-semi-arid-regions-worldwide,](#)
304 [the-need-of-taking-into-account-the-mineralogical-diversity-of-the-soil-composition-at-the-global-scale,](#)
305 [and-finally-by-their-availability-in-sufficient-quantities-for-injection-in-the-chamber.](#) When doing so, we
306 [obtained-a-set-of-twelve-samples-distributed-worldwide-but-mostly-in-Northern-and-Western-Africa](#)
307 [\(Libya, Algeria, Mali, Bodélé\) and the Middle East \(Saudi Arabia and Kuwait\). Individual samples from](#)
308 [the Gobi desert in Eastern Asia, the Namib Desert, the Strzelecki desert in Australia, the Patagonian](#)

deserts in South America, and the Sonoran Desert in Arizona have also been investigated. The selection of these soils and sediments was made out of 137 individual top-soil samples collected in major arid and semi-arid regions worldwide and representing the mineralogical diversity of the soil composition at the global scale. As discussed in Di Biagio et al. (2017), this large sample set was reduced by to a set of 19 samples representing the mineralogical diversity of the soil composition at the global scale and based on their availability in sufficient quantities for injection in the chamber. Because some of the experiments did not produce enough dust to perform good-quality optical measurements, in this paper we present a set of twelve samples distributed worldwide but mostly from Northern and Western Africa (Libya, Algeria, Mali, Bodélé) and the Middle East (Saudi Arabia and Kuwait). Individual samples from the Gobi desert in Eastern Asia, the Namib Desert, the Strzelecki desert in Australia, the Patagonian deserts in South America, and the Sonoran Desert in Arizona have also been investigated.

3.1. Elemental composition and iron oxide content

A total of 41 filters including 15 polycarbonate filters (12 samples and 3 blanks) and 25 quartz filters (12 for the total fraction, 10 for the fine fraction and 3 blanks) were collected for analysis.

The dust mass concentration found by gravimetric analysis varied between $50 \mu\text{g m}^{-3}$ and 5mg m^{-3} , in relatively good agreement with the dust mass concentrations, MC_{dust} , from (Equation 4), based on X-ray fluorescence analysis: the slope of the linear regression between the calculated and the gravimetric values of MC_{dust} is 0.90 with $R^2 = 0.86$.

Di Biagio et al. (2017) showed that clays are the most abundant mineral phases, together with quartz and calcite, and that significant variability exists as function of the compositional heterogeneity of the parent soils. Here we use the Fe/Ca and Si/Al elemental ratios obtained from X-ray fluorescence analysis to discriminate the origin of dust samples. These ratios have been extensively used in the past to discriminate the origin of African dust samples collected in the field (Chiapello et al., 1997; Formenti et al., 2011; Formenti et al., 2014a). The values obtained during our experiments are reported in Table 3. There is a very good correspondence between the values obtained for the Mali, Libya, Algeria, Mauritania and (to a lesser extent) Morocco experiments to values found in environmental aerosol samples by Chiapello et al. (1997) and Formenti et al. (2011; 2014a). These authors indicate that dust from local erosion of Sahelian soils, such as from Mali, have Si/Al ratios in the range of 2-2.5 and Fe/Ca ratios in the range 3-20, depending on the time proximity to the erosion event. Dust from sources in the Sahara, such as Libya and Algeria, show Si/Al ratios in the range of 2-3 and Fe/Ca ratios in the range

339 0.7-3, whereas dust from Morocco has Si/Al ratios around 3 and Fe/Ca ratios around 0.4. The only major
340 difference is observed for the Bodélé experiment, for which the Fe/Ca ratio is enriched by a factor of 6
341 with respect to the values of 1 found during ~~to~~ the field observations (Formenti et al., 2011; ~~Formenti et~~
342 ~~al., 2014a~~). This could reflect the fact that the Bodélé aerosol in the chamber is generated from a sedi-
343 ment sample and not from a soil. As a matter of fact, the Bodélé sediment sample ~~is constituted~~ consists
344 of by a very fine powder which becomes very easily airborne. ~~Henceforth, and contrary to the soil sam-~~
345 ~~ples, this~~ This powder is likely to be injected in the chamber with little or no size fractionation. ~~Hence-~~
346 ~~forth, the aerosol generated from it~~ As a consequence, should have a closer ~~the~~ composition to the
347 original powder of the aerosol collected in the chamber could reflect more that of the parent sedimentary
348 soil than ~~the not the~~ other samples. On the other hand, Bristow et al. (2010) and Moskowitz et al. (2016)
349 showed ed that the iron content and speciation of the Bodélé sediments is very heterogeneous at the source
350 scale. For samples from areas other than ~~non-~~ northern African ~~samples~~, the largest variability is observed
351 for the Fe/Ca values, ranging from 0.1 to 8, whereas the Si/Al ratio varied only between 2.5 and 4.8. In
352 this case, values are available in the literature for comparison (e.g., Cornille et al., 1990; Reid et al.,
353 1994; Eltayeb et al., 2001; Lafon et al., 2006; Shen et al., 2007; Radhi et al., 2010; 2011; Formenti et
354 al., 2011; 2014a; Scheuvens et al., 2013, and references within). Values in the PM_{2.5} fraction are very
355 consistent with those obtained in the PM_{10.6}: their linear correlation has a slope of 1.03 (± 0.05) and a R^2
356 equal to 0.97, suggesting that the elemental composition is relatively size -independent.

357 The mass fraction of total Fe ($MC_{Fe\%}$ from Equation 5), also reported in **Table 3**, ranged from 2.8 (Na-
358 mibia) to 7.3% (Australia), ~~values found for the Namibia and the Australia samples, respectively. This~~
359 These are in the range ~~is in good agreement with of~~ values reported in the literature, taking into account
360 that differences might be also due to the method (direct measurement/calculation) and/or the size fraction
361 over which the total dust mass concentration is estimated (Chiapello et al., 1997; Reid et al., 1994; 2003;
362 Derimian et al., 2008; Formenti et al., 2001; 2011; 2014a; Scheuvens et al., 2013). The agreement of
363 $MC_{Fe\%}$ values obtained by the XRF analysis of polycarbonate filters (Equation 5) and those obtained
364 from the XRF analysis of the quartz filters, normalized to the measured gravimetric mass is well within
365 10% (~~that is,~~ the percent error of each estimate). ~~An the e-~~ Exceptions are the samples ~~of from~~ Bodélé
366 and Algeria, for which the values obtained from the analysis of the quartz filters are significantly lower
367 than those obtained from the nuclepore filters (3.1% versus 4.1% for Bodélé and 4.3% versus 6.8% for
368 Algeria). We treat that as an additional source of error in the rest of the analysis, and add it to the total
369 uncertainty. In the PM_{2.5} fraction, the content of iron is more variable, ranging from 4.4% (Morocco) to

370 33.6% (Mali), showing a size dependence. A word of caution on this conclusion ~~as is that~~ the two esti-
371 mates are not necessarily consistent in the way that the total dust mass is estimated (from Equation 4 for
372 the PM_{10.6} fraction and by gravimetric weighing ~~for~~ the PM_{2.5}).

373 Finally, between 11 and 47% of iron in the samples can be attributed to iron oxides, in variable propor-
374 tions between hematite and goethite. The iron oxide fraction of total Fe in this study is ~~on~~ at the lower
375 end of the range (36-72%) estimated for field dust samples of Saharan/Sahelian origin (Formenti et al.
376 2014b). The highest value of Formenti et al. (2014b), obtained for a sample of locally-emitted dust col-
377 lected at the Banizoumbou station in the African Sahel, is anyhow in excellent agreement with the value
378 of 62% obtained for an experiment (not shown here) using a soil collected in the same area. Likewise,
379 the proportions between hematite and goethite (not shown) are reproduced, showing that goethite is more
380 abundant than hematite. The mass fraction of iron oxides ($MR_{Fe\ ox\%}$), estimated from Equation 8 and
381 shown in Table 3, ranges between 0.7% (Kuwait) ~~to~~ and 3.6% (Australia), which is in the range of
382 available field estimates (Formenti et al., 2014a; Moskowitz et al., 2016). For China, our value of $MR_{Fe\ ox\%}$
383 $ox\%$ is lower by almost a factor of 3 ~~in comparison with~~ compared to that obtained on ~~the same~~ of the
384 same origin sample by Alfaro et al. (2004) (0.9% against 2.8%), whereas on a sample from Niger (~~how-~~
385 ~~ever~~ not considered in this study) our estimates and that by Alfaro et al. (2004) agree perfectly agree
386 (5.8%). A possible underestimate of the iron oxide fraction for samples other than those from the Sahara-
387 Sahel area could be due to the fact that - opposite to the experience of Formenti et al. (2014b) - the linear
388 deconvolutions of the XANES spectra were not always satisfactory (see Figure S1 in the supplementary).
389 This resulted in a significant residual between the observed and fitted XANES spectra. ~~Indeed~~ In fact,
390 the mineralogical reference for hematite is obtained from a soil from Niger (Table 1) and might not be
391 fully suitable for representing aerosols of different origins. Additional differences could arise from dif-
392 ferences in the size distributions of the generated aerosol. As a matter of fact, the number fraction of
393 particles in the size classes above 0.5 μm in diameter is are different in the dust aerosol generated in the
394 Alfaro et al. (2004) study ~~with respect~~ compared to ours. In the study by Alfaro et al. (2004), the number
395 fraction of particles is lowest in the 0.5-0.7 size class and highest between 1 and 5 μm . ~~On the contrary~~ In
396 contrast, in our study the number fraction is lowest in the 1-2 μm size range and highest between 0.5
397 and 0.7 μm . These differences could ~~yield~~ either be due to differences in the chemical composition
398 and/or ~~to a difference~~ in the total mass in the denominator of Equation 8.

399 **34.2. Spectral and size -variability of the mass absorption efficiency**

400 The spectral mass absorption efficiency (MAE) at 375, 407, 532, 635, and 850 nm for the PM_{10.6} and
401 the PM_{2.5} dust fractions are summarized in **Table 4** and displayed in **Figure 3**. Regardless of particle
402 size, the MAE values decrease with increasing wavelength (almost one order of magnitude between 375
403 and 850 nm), and display a larger variability at shorter wavelengths. The MAE values for the PM_{10.6}
404 range from $37 (\pm 3) 10^{-3} \text{ m}^2 \text{ g}^{-1}$ to $135 (\pm 11) 10^{-3} \text{ m}^2 \text{ g}^{-1}$ at 375 nm, and from $1.3 (\pm 0.1) 10^{-3} \text{ m}^2 \text{ g}^{-1}$ to 15
405 $(\pm 1) 10^{-3} \text{ m}^2 \text{ g}^{-1}$ at 850 nm. Maxima are found for the Australia and Algeria samples, whereas the minima
406 are for Bodélé and Namibia, respectively at 375 and 850 nm. In the PM_{2.5} fraction, the MAE values
407 range from $95 (\pm 8) 10^{-3} \text{ m}^2 \text{ g}^{-1}$ to $711 (\pm 70) 10^{-3} \text{ m}^2 \text{ g}^{-1}$ at 375 nm, and from $3.2 (\pm 0.3) 10^{-3} \text{ m}^2 \text{ g}^{-1}$ to 36
408 $(\pm 3) 10^{-3} \text{ m}^2 \text{ g}^{-1}$ at 850 nm. Maxima at both 375 and 850 nm are found for the Morocco sample, whereas
409 the minima are for Algeria and Namibia, respectively. The MAE values for mineral dust resulting from
410 this work are ~~in~~ relatively in good agreement with the estimates available in the literature (Alfaro et al.,
411 2004; Linke et al., 2006; Yang et al., 2009; Denjean et al., 2016), reported in **Table 5**. For the China
412 Ulah Buhn sample, Alfaro et al. (2004) reported $69.1 10^{-3}$ and $9.8 10^{-3} \text{ m}^2 \text{ g}^{-1}$ at 325 and 660 nm, respec-
413 tively. The former is lower than the value of $99 10^{-3} \text{ m}^2 \text{ g}^{-1}$ that we obtain by extrapolating our measure-
414 ment at 375 nm. Likewise, our values for the Morocco sample are higher than reported by Linke et al.
415 (2006) at 266 and 660 nm. Conversely, the agreement with the estimates of Yang et al. (2009) for mineral
416 dust locally re-suspended in Xianghe, near Beijing (China) is very good at all wavelengths between 375
417 and 880 nm. As expected, the MAE values for mineral dust resulting from this work are almost one
418 order of magnitude smaller than for other absorbing aerosols. For black carbon, MAE values are in the
419 range of $6.5\text{--}7.5 \text{ m}^2 \text{ g}^{-1}$ at 850 nm (Bond and Bergstrom, 2006; Massabò et al., 2016), and ~~vary-decrease~~
420 in a linear way with the logarithm of the ~~inversely with~~ wavelength. For brown carbon, the reported
421 MAE range between $2.3\text{--}7.0 \text{ m}^2 \text{ g}^{-1}$ at 350 nm (Chen and Bond, 2010; Kirchstetter et al., 2004; Massabò
422 et al., 2016), $0.05\text{--}1.2 \text{ m}^2 \text{ g}^{-1}$ at 440 nm (Wang et al., 2016) and $0.08\text{--}0.72 \text{ m}^2 \text{ g}^{-1}$ at 550 nm (Chen and
423 Bond, 2010).

424 The analysis of **Table 4** indicates that, at every wavelength, the MAE values in the PM_{2.5} fraction are
425 equal or higher than those for PM_{10.6}. The PM_{2.5}/PM_{10.6} MAE ratios reach values of 6 for the Mali sam-
426 ple, but are mostly in the range 1.5-3 for the ~~remaining-other~~ aerosols. The vValues decrease with wave-
427 length up to 635 nm, whereas at 850 nm they have values comparable to those at 375 nm. The observed
428 size ~~-~~dependence of the MAE values is consistent with the expected behavior of light absorption of
429 particles in the Mie and geometric optical regimes that ~~concern-are relevant for~~ the two size fractions.
430 Light ~~-~~absorption of particles of sizes s smaller or equivalent to the wavelength is proportional to their

431 bulk volume, whereas for larger particles absorption occurs on their surface only (Bohren and Huffmann,
432 1983). On the other hand, the size-resolved measurements of Lafon et al. (2006) show that the proportion
433 (by volume) of iron oxides might be higher in the coarse than in the fine fraction, which would counteract
434 the size-dependence behavior of MAE. To validate the observations, we calculated the spectrally-re-
435 solved MAE values in the two size fractions using the Mie code for homogeneous spherical particles
436 (Bohren and Huffmann, 1983) and the number size distribution estimated by (Di Biagio et al.,
437 [2016\(2017\)](#)) and averaged over the duration of filter sampling. We estimated the dust complex refractive
438 index as a volume-weighted average of a non-absorbing dust fraction having the refractive index of
439 kaolinite, [the](#) dominant mineral in our samples (see Di Biagio et al., [20162017](#)), from Egan et Hilgeman
440 (1979) and an absorbing fraction estimated from the mass fraction of iron oxides and having the refrac-
441 tive index of hematite (Bedidi and Cervelle, 1993). [The r](#)Results of this calculation indicate that the
442 observed size-[dependent](#) behavior is well reproduced at all wavelengths, even in the basic hypothesis
443 that the mineralogical composition does not change with size. The only exception is 850 nm, where at
444 times, PM_{2.5}/PM_{10.6} MAE ratio is much higher than expected theoretically. We attribute that to the rela-
445 tively high uncertainty affecting the absorbance measurements at this wavelength, where the signal-to-
446 noise ratio is low. Indeed, the two sets of values (MAE in the PM_{2.5} fraction and MAE in the PM_{10.6}
447 fraction) are not statistically different according to a two-pair t-test (0.01 and 0.05 level of confidence),
448 confirming that any attempt of differentiation [of](#) the size-[dependence](#) at this wavelength would require
449 a stronger optical signal.

450 The analysis of the spectral dependence, using [a-the](#) power-law function fit [as-\(from](#) Equation 2), pro-
451 vides [with](#) the values of the Angstrom Absorption Exponent (AAE), also reported in **Table 4**. Contrary
452 to the MAE values, there is no statistically significant size-[dependence](#) of the AAE values, ranging from
453 2.5 (± 0.2) to 4.1 (± 0.3), with an average of 3.3 (± 0.7), for the PM_{10.6} size fraction and between 2.6 (\pm
454 0.2) and 5.1 (± 0.4), with an average of 3.5 (± 0.8), for the PM_{2.5} fraction. Our values are in the range of
455 those published in the [open](#)-literature (Fialho et al., 2005; Linke et al., 2006; Müller et al., 2009; Petzold
456 et al., 2009; Yang et al., 2009; Weinzierl et al., 2011; Moosmüller et al., 2012; Denjean et al., 2016),
457 shown in **Table 5**. AAE values close to 1.0 are found for urban aerosols where fossil fuels combustion
458 is dominant, while AAE values for brown carbon (BrC) from incomplete combustion are in the range
459 3.5-4.2 (Yang et al., 2009; Chen et al., 2015; Massabò et al., 2016).

460 Finally, **Figure 4** shows correlations between [the](#) MAE values in the PM_{10.6} fraction (Figure [34.a](#)) and
461 in the PM_{2.5} fraction (Figure [34.b](#)) and the estimated percent mass fraction of iron and iron oxides

462 ($MC_{Fe\%}$ and $MC_{Fe\ ox\%}$), respectively. Regardless of the size fraction, ~~t~~The correlation between the MAE
463 values and the percent mass of total elemental iron are ~~satisfactory. Higher higher correlations are ob-~~
464 ~~tained~~ at 375, 407 and 532 nm, ~~and in the $PM_{2.5}$ fraction, where a linear correlation with R^2 up to 0.94~~
465 ~~are obtained~~. Best correlations are obtained when forcing the intercept to zero, indicating that elemental
466 iron fully accounts for the measured absorption. At these wavelengths, linear correlations with the mass
467 fraction of iron oxides are ~~loose-low~~ in the $PM_{10.6}$ mass fraction (R^2 up to 0.38-0.62), but ~~again satisfac-~~
468 ~~tory~~ ~~higher~~ in the $PM_{2.5}$ fraction (R^2 up to 0.83-0.99), where, ~~whenever~~ ~~however~~, one should keep in mind
469 that they have been established only indirectly by considering the ratio of iron oxides to elemental iron
470 independent of size. At 660 and 850 nm, little or no robust correlations ~~are is-~~ obtained, often ~~based~~ on
471 very few data points and with very low MAE values. It is noteworthy that, in both size fractions, the
472 linear correlation yields a non-zero intercept ~~is obtained~~, indicating ~~a contribution from minerals~~ other
473 ~~minerals but~~ ~~than~~ iron oxides ~~account to~~ ~~for~~ the measured absorption.

474 **4.5. Conclusive remarks**

475 In this paper, we reported ~~new~~ laboratory measurements of the shortwave mass absorption efficiency
476 (MAE) of mineral dust of different origins ~~s~~ and as a function of size and wavelength in the 375-850 nm
477 range. ~~Results-Our results have been~~ ~~were~~ obtained in the CESAM simulation chamber using ~~generated~~
478 mineral dust ~~generated~~ from natural parent soils, ~~in combination with~~ ~~and~~ optical and gravimetric anal-
479 ysis on extracted samples.

480 Our results can be summarized as follows: at 375 nm, the MAE values are lower for the $PM_{10.6}$ mass
481 fraction (range 37-135 $10^{-3} \text{ m}^2 \text{ g}^{-1}$) than for the $PM_{2.5}$ ~~fraction~~ (range 95-711 $10^{-3} \text{ m}^2 \text{ g}^{-1}$), and vary oppo-
482 site to wavelength as λ^{-AAE} , where AAE (Angstrom Absorption Exponent) averages between 3.3-3.5
483 regardless of size fraction. These results deserve some ~~conclusive-concluding~~ comments:

- 484 • The size ~~-~~dependence, ~~yielding-characterized by~~ significantly higher MAE values in the fine
485 fraction ($PM_{2.5}$) than ~~for the in the bulk ($PM_{10.6}$)~~ aerosol, indicates that light ~~-~~absorption by min-
486 eral dust can be important even during atmospheric transport over heavil~~y~~ polluted regions, ~~when~~
487 ~~where~~ dust concentrations are significantly lower than at emission. This can be shown by com-
488 paring the aerosol absorption optical depth (AAOD) at 440 nm for China, a well-known mixing
489 region of mineral dust and pollution (e.g., Yang et al., 2009; Laskin et al., 2014; Wang et al.,
490 2013), ~~as well as offshore western Africa where large urban centers are downwind of dust~~
491 ~~transport areas (Petzold et al., 2011)~~. Laskin et al. (2014) reports that the average AAOD in ~~China~~

492 ~~the area~~ is of the order of 0.1; for carbonaceous absorbing aerosols (sum of black and brown
493 carbon; [Andreae and Gelencsér, 2006](#)). This is lower or comparable to the AAOD of 0.17 and
494 0.11 at 407 nm (~~fine and~~ total ~~and fine~~ mass fractions, respectively) that we ~~obtain~~ derive by a
495 simple calculation ($AAOD = MAE \times MC_{dust} \times H$), ~~where from~~ MAE ~~are the~~ values estimated in
496 this study, ~~(MC_{dust})~~ the dust mass concentrations typically observed in ~~the area~~ urban area of
497 [Beijing](#) during dust storms (Sun et al., ~~2004~~2005), and H , a scale height factor of 1 km).

498 • The spectral variability of the dust MAE values, represented by the AAE parameter, is equal in
499 the PM_{2.5} and PM_{10.6} mass fractions. This suggests that, for a given size distribution, the possible
500 variation of dust composition with size ~~does~~ not affect in a significant way the spectral behavior
501 of the absorption properties. Our average value for AAE is 3.3 ± 0.7 , higher than for black carbon,
502 but in the same range ~~than as~~ light-absorbing organic (brown) carbon. As a result, depending on
503 the environment, there can be some ambiguity in apportioning the AAOD based on spectral de-
504 pendence. Bahadur et al. (2012) and Chung et al. (2012) couple the AAE and the spectral de-
505 pendence of the total AOD (~~and/or its scattering fraction only~~) to overcome this problem. Still,
506 Bahadur et al. (2012) show that there is an overlap in the scatterplots of the spectral dependence
507 of the scattering and absorption fractions of the AOD based on ~~an~~ analysis of ground-based re-
508 mote sensing data for mineral dust, urban, and non-urban fossil fuel over California. A closer
509 look ~~should be taken at~~ observations in mixing areas where biomass burning ~~aerosols may~~
510 have different chemical composition and/or mineral dust has heavy loadings ~~should be given~~ in
511 order to generalize the clear separation observed in the spectral dependences of mineral dust and
512 biomass burning (Bahadur et al., 2012). This aspect is relevant to the development of remote
513 sensing ~~retrievals~~ of light-~~absorption by~~ aerosols from space, and their assimilation in climate
514 models (Torres et al., 2007; Buchard et al., 2015; Hammer et al., 2016).

515 • There is an important sample-to-sample variability in our dataset of MAE values for mineral dust
516 aerosols. At 532 nm, our ~~estimated average~~ MAE ~~values average to are at~~ $34 \pm 14 \text{ m}^2 \text{ g}^{-1}$ and 78
517 $\pm 70 \text{ m}^2 \text{ g}^{-1}$ in the PM_{10.6} and PM_{2.5} mass fractions, respectively. Figure 3, showing the correlation
518 with the estimated mass fraction of elemental iron and iron oxides, suggests that this variability
519 could be related to the regional differences of the mineralogical composition of the parent soils.
520 These observations lead to ~~different considerations~~ further conclusions. To start with, our study
521 reinforces the need for regionally-resolved representation of the light-~~absorption~~ properties of

522 mineral dust in order to improve the representation of its effect on climate. As a matter of fact,
523 the natural variability of the absorption properties that we obtain from our study is in the range
524 50-100%, even when we limit ourselves to smaller spatial scales, for example those ~~of from~~ north
525 Africa (samples from Libya, Algeria, Mali and Bodélé). ~~This is far above the $\pm 5\%$ sensitivity~~
526 ~~factor used by Solmon et al. (2008) to vary the single scattering albedo (as a proxy of absorption)~~
527 ~~of mineral dust over western Africa, and to show how this could drastically change the climate~~
528 ~~response in the region. As a comparison, Solmon et al. (2008) showed that varying the single~~
529 ~~scattering albedo of mineral dust over western Africa by $\pm 5\%$, that is, varying the co-albedo (or~~
530 ~~absorption) by 45% (0.1 ± 0.045) could drastically change the climate response in the region.~~

531 The question is then “how to represent this regional variability?” ~~As Like~~ Moosmüller et al.
532 (2012) ~~and Engelbrecht et al. (2016)~~, we found that elemental iron is a very good proxy for the
533 MAE, especially in the PM_{2.5} fraction, where iron-bearing absorbing minerals (hematite, goe-
534 thite, illite, smectite clays) ~~would beare~~ more concentrated. In the coarse fraction, Ca-rich min-
535 erals, quartz, and feldspars could also play a role, and that could result in the observed lower~~ed~~
536 correlation (although adding a term proportional to elemental Ca does not ~~ameliorate-improve~~
537 the ~~correlation-result~~ in the present study). The correlation of the spectral MAE values with the
538 iron oxide fraction is satisfactory but rather noisy, also owing to some uncertainty in the quanti-
539 fication of iron oxides from X-Ray ~~Absorption-absorption~~ measurements. In this case, the inter-
540 cept is significantly different from zero, again indicating that a small but ~~clear-distinct~~ fraction
541 of absorption is due to minerals other than iron oxides. There are contrasting results on this topic:
542 Alfaro et al. (2004) found an excellent correlation between MAE and the iron oxide content,
543 whereas Klaver et al. (2011) found that the single scattering albedo (representing the capacity of
544 an aerosol population to absorb light ~~with respect in relation~~ to extinction) was almost independ-
545 ent on the mass fraction of iron oxides. Moosmüller et al. (2012) disagreed, pointing out ~~to~~ the
546 uncertainty in the correction procedure of the measurement of absorption by Klaver et al. (2011).
547 As a matter of fact, Klaver et al. (2011) and Alfaro et al. (2004) used the same correction proce-
548 dure. It is more likely that the lack of correlation found in Klaver et al. (2011) is due to the fact
549 that ~~other~~ minerals ~~other~~ than iron oxides contribute to absorption, in particular at their working
550 wavelength (567 nm), where the absorption efficiency of iron oxides starts to weaken. Clearly,
551 the linear correlation between elemental iron in mineral dust and its light-absorption properties

552 could ease the application and validation of climate models that are now starting to include in-
553 cluding the representation of the mineralogy (Perlwitz et al., 2015a; 2015b; Scanza et al., 2015).
554 Also, they-this would facilitate detecting source regions based on remote sensing of dust absorp-
555 tion in the UV-VIS spectral region (e.g., Hsu et al., 2004). However, such a quantitative relation-
556 ship cannot be uniquely determined from these studies, including the present one, which use
557 different ways of estimating elemental iron, iron oxides, and the total dust mass. A more robust
558 estimate should be obtained fromby estimating the imaginary parts of the complex refractive
559 indices associated to-with these measurements of absorption, and their dependence on the min-
560 eralological composition.

561 **Author contributions**

562 L. Caponi, P. Formenti, D. Massabò, P. Prati, C. Di Biagio, and J. F. Doussin designed the chamber
563 experiments and discussed the results. L. Caponi and C. Di Biagio realized-conducted the experiments
564 with contributions by M. Cazaunau, E. Pangui, P. Formenti, and J.F. Doussin. L. Caponi, D. Massabò
565 and P. Formenti performed the full data analysis with contributions by C. Di Biagio, P. Prati and J.F.
566 Doussin. L. Caponi, P. Formenti and S. Chevallier performed the XRF measurements. P. Formenti and
567 G. Landrot performed the XAS measurements. D. Massabò performed the MWAA and the gravimetric
568 measurements. M. O. Andreae, K. Kandler, T. Saeed, S. Piketh, D. Seibert, and E. Williams collected
569 the soil samples used for experiments. L. Caponi, P. Formenti, D. Massabò and P. Prati wrote the man-
570 uscript with comments from all co-authors.

571 **Acknowledgements**

572 The RED-DUST project was supported by the French national programme LEFE/INSU, by the EC
573 within the I3 project “Integration of European Simulation Chambers for Investigating Atmospheric Pro-
574 cesses” (EUROCHAMP 2020, grant agreement n. 730997), by the Institut Pierre Simon Laplace (IPSL),
575 and by OSU-EFLUVE (Observatoire des Sciences de l’Univers-Enveloppes Fluides de la Ville à l’Ex-
576 obiologie) through dedicated research funding. This work has received funding from the European Un-
577 ion’s Horizon 2020 research and innovation programme through the EUROCHAMP-2020 Infrastructure
578 Activity under grant agreement no. 730997. It was supported by the French national programme
579 LEFE/INSU, by the OSU-EFLUVE (Observatoire des Sciences de l’Univers-Enveloppes Fluides de la
580 Ville à l’Exobiologie) through dedicated research funding, by the CNRS-INSU by supporting CESAM
581 as national facility, and by the project of the TOSCA program of the CNES (Centre National des Etudes

582 [Spatales](#)). C. Di Biagio was supported by the CNRS via the Labex L-IPSL. M. O. Andreae was sup-
583 ported [by funding from King Saud University and the Max Planck Society](#)~~by the Max Society and by~~
584 [King Saud University](#). The mobility of researchers between Italy and France was supported by the PICS
585 programme MedMEx of the CNRS-INSU. The authors acknowledge the CNRS-INSU for supporting
586 CESAM as national facility. K. Kandler acknowledges support from the Deutsche Forschungsgemein-
587 schaft (DFG grant KA 2280/2-1). [The authors strongly thank the LISA staff who participated in the](#)
588 [collection of the soil samples from Patagonia and the Gobi desert used in this study, and the two anon-](#)
589 [ymous reviewers for useful comments on the manuscript. P. Formenti thanks Dr. Hans Moosmüller](#)
590 [\(Desert Research Institute, Reno, Nevada\) for providing with fruitful](#) ~~elements~~[suggestions for-of im-](#)
591 [provement and discussion to the paper.](#)

592 **References**

- 593 Alfaro, S. C., Lafon, S., Rajot, J. L., Formenti, P., Gaudichet, A., and Maille, M., Iron oxides and light
594 absorption by pure desert dust: An experimental study, *J. Geophys. Res. Atmos.*, 109, D08208,
595 doi:10.1029/2003JD004374, 2004.
- 596 [Andreae, M. O., and Gelencsér, A., Black carbon or brown carbon? The nature of light-absorbing car-](#)
597 [bonaceous aerosols: *Atmos. Chem. Phys.*, 6, 3131-3148, 2006.](#)
- 598 [Anderson, T. L. and Ogren, J. A., Determining aerosol radiative properties using the TSI 3563 integrat-](#)
599 [ing nephelometer, *Aerosol. Sci. Technol.*, 29, 57–69, 1998.](#)
- 600 [Andrews, E., Sheridan, P. J., Fiebig, M., McComiskey, A., Ogren, J. A., Arnott, P., Covert, D., Elleman,](#)
601 [R., Gasparini, R., Collins, D., Jonsson, H., Schmid, B., and Wang J., Comparison of methods](#)
602 [for deriving aerosol asymmetry parameter, *J. Geophys. Res.*, 111, D05S04,](#)
603 [doi:10.1029/2004JD005734, 2006.](#)
- 604 [Arnott, W., Hamasha, K., Moosmüller, H., Sheridan, P. J., and Ogren, J. A., Towards aerosol light-](#)
605 [absorption measurements with a 7 wavelength aethalometer: Evaluation with a photoacoustic](#)
606 [instrument and 3 wavelength nephelometer, *Aerosol Sci Tech.*, 39\(1\), 17–29, 2005.](#)
- 607 Bahadur, R., P. S. Praveen, Y. Xu, and V. Ramanathan, Solar absorption by elemental and brown carbon
608 determined from spectral observations, *PNAS*, 109(43), 17366-17371, 2012.
- 609 Balkanski, Y., Schulz, M., Claquin, T., and Guibert, S., Re-evaluation of Mineral aerosol radiative forc-
610 ing suggests a better agreement with satellite and AERONET data, *Atmos. Chem. Phys.*, 7, 81–
611 95, doi:10.5194/acp-7-81-2007, 2007.
- 612 Bedidi, A., and Cervelle B., Light scattering by spherical particles with hematite and goethitelike optical
613 properties: Effect of water impregnation, *J. Geophys. Res.*, 98(B7), 11941–11952,
614 doi:10.1029/93JB00188, 1993.
- 615 Bond, T.C. and Bergstrom, R.W., Light absorption by carbonaceous particles: an investigative review.
616 *Aerosol Sci. Technol.* 40, 27e67, 2006.

- 617 Boucher, O., Randall, D., Artaxo, P., Bretherton, C., Feingold, G., Forster, P., Kerminen, V.-M., Kondo,
618 Y., Liao, H., Lohmann, U., Rasch, P., Satheesh, S.K., Sherwood, S., Stevens B., and Zhang X.
619 Y., Clouds and Aerosols. In: Climate Change 2013: The Physical Science Basis. Contribution of
620 Working Group I to the Fifth Assessment Report of the Intergovernmental Panel on Climate
621 Change [Stocker, T.F., D. Qin, G.-K. Plattner, M. Tignor, S.K. Allen, J. Boschung, A. Nauels,
622 Y. Xia, V. Bex and P.M. Midgley (eds.)]. Cambridge University Press, Cambridge, United King-
623 dom and New York, NY, USA, 2013.
- 624 Brégonzio-Rozier, L., F. Siekmann, C. Giorio, E. Pangui, S. B. Morales, B. Temime-Roussel, Aline
625 Gratien, V. Michoud, S. Ravier, A. Tapparo, A. Monod, Jean-Francois Doussin, Gaseous prod-
626 ucts and secondary organic aerosol formation during long term oxidation of isoprene and meth-
627 acrolein, *Atmos. Chem. Phys.*, 15, 2953-2968, 2015.
- 628 Brégonzio-Rozier L., C. Giorio, F. Siekmann, E. Pangui, S. B. Morales, B. Temime-Roussel, A. Gratien,
629 V. Michoud, M. Cazaunau, H. L. DeWitt, A. Tapparo, A. Monod and J.-F. Doussin, Secondary
630 Organic Aerosol formation from isoprene photooxidation during cloud condensation-evaporation
631 cycles, *Atmospheric Chemistry and Physics*, 16: 1747-1760, 2016.
- 632 Bristow, C. S., Hudson-Edwards, K. A., and Chappell, A.: Fertilizing the Amazon and equatorial Atlan-
633 tic with West African dust, *Geophys. Res. Lett.*, 37, L14807, 10.1029/2010GL043486, 2010.
- 634 Buchard, V., da Silva, A. M., Colarco, P. R., Darmenov, A., Randles, C. A., Govindaraju, R., Torres,
635 O., Campbell, J., and Spurr, R.: Using the OMI aerosol index and absorption aerosol optical
636 depth to evaluate the NASA MERRA Aerosol Reanalysis, *Atmos. Chem. Phys.*, 15, 5743–5760,
637 doi:10.5194/acp-15-5743-2015, 2015.
- 638 Chen, L.-W.A., Chow, J.C., Wang, X.L., Robles, J.A., Sumlin, B.J., Lowenthal, D.H., Zimmermann, R.,
639 Watson, J.G., Multi-wavelength optical measurement to enhance thermal/optical analysis for car-
640 bonaceous aerosol, *Atmos. Meas. Tech.* 8, 451-461, 2015.
- 641 Chen, Y. and Bond, T. C., Light absorption by organic carbon from wood combustion, *Atmos. Chem.*
642 *Phys.*, 10:1773–1787, 2010.
- 643 [Chiapello, I., G. Bergametti, B. Chatenet, P. Bousquet, F. Dulac, and E. Santos Suares, Origins of Afri-
644 can dust transported over the northeastern tropical Atlantic., *J. Geophys. Res.*, 102\(D12\), 13701-
645 13709, 1997.](#)
- 646 Chiapello, I., Dust Observations and Climatology, in P. Knippertz and J.-B.W. Stuut (eds.), *Mineral
647 Dust: A Key Player in the Earth System*, DOI 10.1007/978-94-017-8978-3__7, ©Springer Sci-
648 enceCBusiness Media, Dordrecht, 2014.
- 649 Chung, C. E., V. Ramanathan, and D. Decremmer, Observationally constrained estimates of carbonaceous
650 aerosol radiative forcing, *PNAS*, 109(29), 11624-11629, 2012.
- 651 Coakley, J.A. and Chylek, P., The two-stream approximation in radiative transfer: Including the angle
652 of incident radiation, *J. Atmos. Sci.* 32, 409 – 418, 1975.
- 653 Colarco, P. R., O. B. Toon, O. Torres, and F. J. Rasch, Determining the UV imaginary part of refractive
654 index of Saharan dust particles from TOMS data and a three dimensional model of dust transport,
655 *J. Geophys. Res.*, 107(D16), 10.1029/2001JD000903, 2002.

- 656 [Collaud Coen, M., Weingartner, E., Apituley, A., Ceburnis, D., Fierz-Schmidhauser, R., Flentje, H.,](#)
657 [Henzing, J.S., Jennings, S.G., Moerman, M., Petzold, A., Schmid, O., Baltensperger, U., Mini-](#)
658 [mizing light absorption measurement artifacts of the Aethalometer: evaluation of five correction](#)
659 [algorithms, Atmos. Meas. Tech. 3, 457-474, 2010.](#)
- 660 Denjean, C., Paola Formenti, Benedicte Picquet-Varrault, Edouard Pangui, Pascal Zapf, Y. Katrib, C.
661 Giorio, A. Tapparo, A. Monod, B. Temime-Roussel, P. Decorse, C. Mangeney, Jean-Francois
662 Doussin, Relating hygroscopicity and optical properties to chemical composition and structure
663 of secondary organic aerosol particles generated from the ozonolysis of α -pinene, Atmos. Chem.
664 Phys., 15, 3339-3358, 2015a.
- 665 Denjean, C., Paola Formenti, Benedicte Picquet-Varrault, Marie Camredon, Edouard Pangui, Pascal
666 Zapf, Katrib, Y., Giorio, C., Tapparo, A., Temime-Roussel, B., Monod, A., Bernard Aumont,
667 Jean-Francois Doussin, Aging of secondary organic aerosol generated from the ozonolysis of α -
668 pinene: effects of ozone, light and temperature, Atmos. Chem. Phys., 15, 883-897,
669 doi:10.5194/acp-15-883-2015, 2015b.
- 670 Denjean, C., Cassola, F., Mazzino, A., Triquet, S., Chevaillier, S., Grand, N., Bourriane, T., Mom-
671 boisse, G., Sellegri, K., Schwarzenbock, A., Freney, E., Mallet, M., and Formenti, P., Size distri-
672 bution and optical properties of mineral dust aerosols transported in the western Mediterranean,
673 Atmos. Chem. Phys., 15, 21607–21669, doi:10.5194/acpd-15-21607-2015, 2015c.
- 674 Denjean, C., *et al.*, Size distribution and optical properties of African mineral dust after intercontinental
675 transport, J. Geophys. Res. Atmos., 121, 7117–7138, doi:10.1002/2016JD024783, 2016.
- 676 Derimian, Y., A. Karnieli, Y. J. Kaufman, M. O. Andreae, T. W. Andreae, O. Dubovik, W. Maenhaut,
677 and I. Koren: The role of iron and black carbon in aerosol light absorption. Atmos. Chem. Phys.,
678 8, 3623–3637, (2008).
- 679 Di Biagio, C., Formenti P., Styler S. A., Pangui E., and Doussin J.-F., Laboratory chamber measurements
680 of the longwave extinction spectra and complex refractive indices of African and Asian mineral
681 dusts, Geophys. Res. Lett., 41, 6289-6297, doi:10.1002/2014GL060213, 2014.
- 682 [Di Biagio, C., Formenti, P., Balkanski, Y., Caponi, L., Cazaunau, M., Pangui, E., Journet, E., Nowak, S., Ca-](#)
683 [quineau, S., Andreae, M. O., Kandler, K., Saeed, T., Piketh, S., Seibert, D., Williams, E., and Doussin,](#)
684 [J.-F.: Global scale variability of the mineral dust long-wave refractive index: a new dataset of in situ](#)
685 [measurements for climate modeling and remote sensing, Atmos. Chem. Phys., 17, 1901-1929,](#)
686 [doi:10.5194/acp-17-1901-2017, 2017.](#)
- 687 [Di Biagio, C., Formenti, P., Balkanski, Y., Caponi, L., Cazaunau, M., Pangui, E., Journet, E., Nowak,](#)
688 [S., Caquineau, S., Andreae, M. O., Kandler, K., Saeed, T., Piketh, S., Seibert, D., Williams, E.,](#)
689 [and Doussin, J.-F.: Global scale variability of the mineral dust longwave refractive index: a new](#)
690 [dataset of in situ measurements for climate modelling and remote sensing, Atmos. Chem. Phys.](#)
691 [Discuss., doi:10.5194/acp-2016-616, in review, 2016.](#)
- 692 Dubovik, O., B. N. Holben, T. F. Eck, A. Smirnov, Y. J. Kaufman, M. D. King, D. Tanre, and I. Slutsker,
693 Variability of absorption and optical properties of key aerosol types observed in worldwide lo-
694 cations, J. Atmos. Sci., 59, 590–608, 2002.
- 695 Egan, W. G. and Hilgeman, T. W.: Optical Properties of Inhomogeneous Materials: Applications to
696 Geology, Astronomy, Chemistry, and Engineering, Academic Press, 235 pp., 1979.

- 697 [Engelbrecht, J. P., Moosmüller, H., Pincock, S., Jayanty, R. K. M., Lersch, T., and Casuccio, G.: Technical note:](#)
698 [Mineralogical, chemical, morphological, and optical interrelationships of mineral dust re-suspensions,](#)
699 [Atmos. Chem. Phys., 16, 10809-10830, doi:10.5194/acp-16-10809-2016, 2016.](#)
- 700 Fialho, P., A.D.A. Hansen, R.E. Honrath, Absorption coefficients by aerosols in remote areas: a new
701 approach to decouple dust and black carbon absorption coefficients using seven-wavelength Ae-
702 thalometer data, *J. Aeros. Sci.*, 36, 267–282, 2005.
- 703 ~~[Filep, Á., Ajtai, T., Utry, N., Pintér, M., Nyilas, T., Takács, S., Máté, Z., Gelencsér, A., Hoffer, A.,](#)~~
704 ~~[Schnaiter, M., Bozóki, Z., and Szabó, G., Absorption spectrum of ambient aerosol and its corre-](#)~~
705 ~~[lation with size distribution in specific atmospheric conditions after a Red Mud Accident, *Aero-*](#)~~
706 ~~[sol Air Qual. Res.](#)~~ 13, 49–59, 2013.
- 707 Formenti, P., S. Nava, P. Prati, S. Chevaillier, A. Klaver, S. Lafon, F. Mazzei, G. Calzolari, and M. Chiari,
708 Self-attenuation artifacts and correction factors of light element measurements by X-ray analysis:
709 Implication for mineral dust composition studies, *J. Geophys. Res.*, 115, D01203,
710 doi:10.1029/2009JD012701, 2010.
- 711 Formenti, P., Rajot, J. L., Desboeufs, K., Saïd, F., Grand, N., Chevaillier, S., and Schmechtig, C., Air-
712 borne observations of mineral dust over western Africa in the summer Monsoon season: spatial
713 and vertical variability of physico-chemical and optical properties, *Atmos. Chem. Phys.*, 11,
714 6387–6410, doi:10.5194/acp-11-6387-2011, 2011.
- 715 Formenti, P., Caquineau, S., Desboeufs, K., Klaver, A., Chevaillier, S., Journet, E. and Rajot, J. L.,
716 Mapping the physico-chemical properties of mineral dust in western Africa: mineralogical com-
717 position, *Atmos. Chem. Phys.*, 14, 10663–10686, doi:10.5194/acp-14-10663-2014, 2014a.
- 718 Formenti, P., Caquineau, S., Chevaillier, S., Klaver, A., Desboeufs, K., Rajot, J. L., Belin, S. and Briois,
719 V.: Dominance of goethite over hematite in iron oxides of mineral dust from western Africa:
720 quantitative partitioning by X-ray Absorption Spectroscopy, *J. Geophys. Res.*, 2014b.
- 721 Hammer, M. S., Martin, R. V., van Donkelaar, A., Buchard, V., Torres, O., Ridley, D. A., and Spurr, R.
722 J. D.: Interpreting the ultraviolet aerosol index observed with the OMI satellite instrument to
723 understand absorption by organic aerosols: implications for atmospheric oxidation and direct ra-
724 diative effects, *Atmos. Chem. Phys.*, 16, 2507-2523, doi:10.5194/acp-16-2507-2016, 2016.
- 725 Hänel, G., Radiation budget of the boundary layer: Part II. Simultaneous measurement of mean solar
726 volume absorption and extinction coefficients of particles, *Beitr. Phys. Atmos.* 60, 241-247,
727 1987.
- 728 Hänel, G., Optical properties of atmospheric particles: complete parameter sets obtained through polar
729 photometry and an improved inversion technique, *Appl. Opt.* 33, 7187-7199, 1994.
- 730 Harrison, R.M., Beddows, D.C.S., Jones, A.M., Calvo, A., Alves, C., and Pio, C., An evaluation of some
731 issues regarding the use of aethalometers to measure woodsmoke concentrations, *Atmos. Envi-*
732 *ron.* 80, 540e548, 2013.
- 733 Haywood, J. M., P. N. Francis, M. D. Glew, and J. P. Taylor, Optical properties and direct radiative
734 effect of Saharan dust: A case study of two Saharan outbreaks using data from the U. K. Met.
735 Office C-130, *J. Geophys. Res.*, 106, 18,417–18,430, 2001.
- 736 Haywood, J., Francis, P., Osborne, S., Glew, M., Loeb, N., Highwood, E., Tanré, D., Myhre, G., For-
737 menti, P., and Hirst, E., Radiative properties and direct radiative effect of Saharan dust measured

- 738 by the C-130 aircraft during Saharan Dust Experiment (SHADE). 1: Solar spectrum, *J. Geophys.*
739 *Res.*, 108(D18), 8577, doi:10.1029/2002JD002687, 2003.
- 740 Hsu, N. C., S.-C. Tsay, M. D. King, and J. R. Herman, *Aerosol Properties Over Bright-Reflecting Source*
741 *Regions*, *IEEE Transactions Geos. Remote Sens.*, 42, 557-569, 2004.
- 742 IPCC 2013, *Climate Change 2013: The Scientific Basis, Summary for Policymakers, Working Group I*
743 *Contribution to the Fifth Assessment Report of the Intergovernmental Panel on Climate Change*,
744 edited by: Stocker, T. F., Qin, D., Plattner, G.-K., Tignor, M. M. B., Allen, S. K., Boschung, J.,
745 Nauels, A., Xia, Y., Bex, V., Midgley, P. M., Cambridge University Press, Cambridge, UK, 2013.
- 746 Journet, E., Balkanski, Y., and Harrison, S. P., A new data set of soil mineralogy for dust-cycle model-
747 ing, *Atmos. Chem. Phys.*, 14, 3801-3816, doi:10.5194/acp-14-3801-2014, 2014.
- 748 Kandler, K., Benker, N., Bundke, U., Cuevas, E., Ebert, M., Knippertz, P., Rodriguez, S., Schütz, L.,
749 and Weinbruch, S.: Chemical composition and complex refractive index of Saharan Mineral Dust
750 at Izaña, Tenerife (Spain) derived by elec-tron microscopy, *Atmos. Environ.*, 41, 8058-8074,
751 10.1016/j.atmosenv.2007.06.047, 2007.
- 752 Kandler, K., Schütz, L., Deutscher, C., Hofmann, H., Jäckel, S., Knippertz, P., Lieke, K., Massling, A.,
753 Schladitz, A., Wein-zierl, B., Zorn, S., Ebert, M., Jaenicke, R., Petzold, A., and Weinbruch, S.,
754 Size distribution, mass concentration, chemical and mineralogical composition, and derived op-
755 tical parameters of the boundary layer aerosol at Tinfou, Morocco, during SAMUM 2006, *Tellus*,
756 61B, 32-50, 10.1111/j.1600-0889.2008.00385.x, 2009.
- 757 Kandler, K., Lieke, K., Benker, N., Emmel, C., Küpper, M., Müller-Ebert, D., Ebert, M., Scheuvs, D.,
758 Schladitz, A., Schütz, L., and Weinbruch, S.: Electron microscopy of particles collected at Praia,
759 Cape Verde, during the Saharan Mineral dust experiment: particle chemistry, shape, mixing state
760 and complex refractive index, *Tellus*, 63B, 475-496, 10.1111/j.1600-0889.2011.00550.x, 2011.
- 761 Karickhoff, S. W. and Bailey, G. W., Optical absorption spectra of clay minerals, *Clays Clay Min.*, 21,
762 59-70, 1973.
- 763 Kirchstetter, T.W., Novakok, T., Hobbs, P.V., Evidence that the spectral dependence of light absorption
764 by aerosols is affected by organic carbon, *J. Geophys. Res.* 109, D21208, 2004.
- 765 Klaver, A., Formenti, P., Caquineau, S., Chevaillier, S., Ausset, P., Calzolari, G., Osborne, S., Johnson,
766 B., Harrison, M., and Dubovik, O., Physico-chemical and optical properties of Sahelian and
767 Saharan mineral dust: in situ measurements during the GERBILS campaign, *Q. J. R. Meteorol.*
768 *Soc.*, DOI:10.1002/qj.889, 2011.
- 769 Knippertz, P., and J.-B. W. Stuut (eds.), *Mineral Dust: A Key Player in the Earth System*, DOI
770 10.1007/978-94-017-8978-3__1, Springer ScienceCBusiness Media Dordrecht, 2014.
- 771 ~~Lack, D. A., and Langridge, J. M., On the attribution of black and brown carbon light absorption using~~
772 ~~the Angström exponent, *Atmos. Chem. Phys.* 13, 10535-10543, 2013.~~
- 773 Lafon, S., J. Rajot, S. Alfaro, and A. Gaudichet, Quantification of iron oxides in desert aerosol, *Atmos.*
774 *Environ.*, 38, 1211-1218, 2004.
- 775 Lafon, S., Sokolik, I.N., Rajot, J.L., Caquineau, S., Gaudichet, A., Characterization of iron oxides in
776 mineral dust aerosols: Implications for light absorption, *J. Geophys. Res.* 111, D21207,
777 DOI:10.1029/2005JD007016, 2006.

- 778 Laskin, J., Laskin, A., Nizkorodov, S. A., Roach, P., Eckert, P., Gilles, M. K., Wang, B., Lee, H. J., and
779 Hu, Q., Molecular Selectivity of Brown Carbon Chromophores, *Environ. Sci. Technol.*, 48,
780 12047–12055, 2014.
- 781 Lau, K. M., K. M. Kim, Y. C. Sud, and G. K. Walker, A GCM study of the response of the atmospheric
782 water cycle of West Africa and the Atlantic to Saharan dust radiative forcing, *Ann. Geophys.*,
783 27, 4023–4037, doi:10.5194/angeo-27-4023-2009, 2009.
- 784 Lazaro, F. J., L. Gutiérrez, V. Barrón, and M. D. Gelado, The speciation of iron in desert dust collected
785 in Gran Canaria (Canary Islands): Combined chemical, magnetic and optical analysis, *Atmos.*
786 *Environ.*, 42(40), 8987-8996, 2008.
- 787 ~~Lewis, K., Arnott, W. P., Moosmüller, H., Wold, C. E., Strong spectral variation of biomass smoke light~~
788 ~~absorption and single scattering albedo observed with a novel dual wavelength photoacoustic~~
789 ~~instrument, *J. Geophys. Res.* 113, D16203, 2008.~~
- 790 ~~Liao, H., and Seinfeld, J.H., Radiative forcing by mineral dust aerosols: Sensitivity to key variables, *J.*
791 ~~*Geophys. Res.*, 103, 31,637–31,645, 1998.~~~~
- 792 Lide, D. R., *CRC Handbook of Chemistry and Physics 1991 – 1992*, CRC Press, Boca Raton, Fla., 1992.
- 793 Linke, C., Möhler, O., Veres, A., Mohácsi, A., Bozóki, Z., Szabó, G., and Schnaiter, M., Optical prop-
794 erties and mineralogical composition of different Saharan mineral dust samples: a laboratory
795 study, *Atmos. Chem. Phys.*, 6, 3315–3323, 2006.
- 796 Loeb, N. G., and W. Su, Direct Aerosol Radiative Forcing Uncertainty Based on a Radiative Perturbation
797 Analysis, *J. Climate*, 23, 5288, 2010.
- 798 Massabó, D., Bernardoni, V., Bove, M.C., Brunengo, A., Cuccia, E., Piazzalunga, A., Prati, P., Valli,
799 G., Vecchi, R., A multi-wavelength optical set-up for the characterization of carbonaceous par-
800 ticulate matter, *J. Aerosol Sci.* 60, 34-46, 2013.
- 801 Massabó, D., Caponi, L., Bernardoni, V., Bove, M.C., Brotto, P., Calzolari, G., Cassola, F., Chiari, M.,
802 Fedi, M.E., Fermo, P., Giannoni, M., Lucarelli, F., Nava, S., Piazzalunga, A., Valli, G., Vecchi,
803 R., Prati, P., Multi-wavelength optical determination of black and brown carbon in atmospheric
804 aerosols, *Atmos. Environ.*, 108, 1-12, 2015.
- 805 Massabò, D., Caponi, L., Bove, M.C., Prati, P., Brown carbon and thermal-optical analysis: A correction
806 based on optical multi-wavelength apportionment of atmospheric aerosols, *Atmos. Environ.*,
807 125, 119-125. doi: 10.1016/j.atmosenv.2015.11.011, 2016.
- 808 ~~McConnell, C.L., E. J. Highwood, H. Coe, P. Formenti, B. Anderson, S. Osborne, S. Nava, and G. Chen,~~
809 ~~Seasonal variations of the physical and optical characteristics of Saharan dust: results from the~~
810 ~~Dust Outflow and Deposition to the Ocean (DODO) Experiment, *J. Geophys. Res.*, 113,~~
811 ~~<http://dx.doi.org/10.1029/2007JD009606>, 2008.~~
- 812 ~~McConnell, C. L., P. Formenti, E. J. Highwood, and M. A. J. Harrison, Using aircraft measurements to~~
813 ~~determine the refractive index of Saharan dust during the DODO Experiments, *Atmos. Chem.*
814 ~~*Phys.*, 10(6), 3081–3098, 2010.~~~~
- 815 Miller, R.L., Tegen, I. and Perlwitz, J.P., Surface radiative forcing by soil dust aerosols and the hydro-
816 logic cycle, *J. Geophys. Res.*, 109, D04203, doi:10.1029/2003JD004085, 2004.

- 817 Miller, R.L., Knippertz, P., Garcia-Pardo, C.P., Perlwitz, J.P., and Tegen, I., Impact of dust radiative
818 forcing upon climate, *Mineral Dust*, 327-357, Springer Netherlands, 2014.
- 819 Ming, Y, Ramaswamy V, and G. Persad, Two opposing effects of absorbing aerosols on global mean
820 precipitation, *Geophys. Res. Lett.* 37, L13701. doi:10.1029/2010GL042895, 2010.
- 821 Moosmüller, H., Chakrabarty, R. K., and W. P. Arnott, Aerosol light absorption and its measurement:
822 A review, *J. Quant. Spectr. Rad. Trans.*, 110, 844–878, 2009.
- 823 Moosmüller, H., Engelbrecht, J. P., Skiba, M., Frey, G., Chakrabarty, R.K., and Arnott, W.P., Single
824 scattering albedo of fine mineral dust aerosols controlled by iron concentration, *J. Geophys. Res.*,
825 117, D11210, doi:10.1029/2011JD016909, 2012.
- 826 Moskowicz, B. M., R. L. Reynolds, H. L. Goldstein, T. S. Berquó, R. F. Kokaly, and C. S. Bristow, Iron
827 oxide minerals in dust-source sediments from the Bodélé Depression, Chad: Implications for
828 radiative properties and Fe bioavailability of dust plumes from the Sahara, *Aeolian Research*, 22,
829 93-106, 2016.
- 830 Müller, T., Schladitz, A., Massling, A., Kaaden, N., Kandler, K., and Wiedensohler, A., Spectral absorp-
831 tion coefficients and imaginary parts of refractive indices of Saharan dust during SAMUM-1,
832 *Tellus B*, 61, 79–95, doi:10.3402/tellusb.v61i1.16816, 2009.
- 833 Patterson, E. M., D. A. Gillette, and B. H. Stockton, Complex index of refraction between 300 and 700
834 nm for Saharan aerosol, *J. Geophys. Res.*, 82, 3153– 3160, 1977.
- 835 Pérez C., S. Nickovic, G. Pejanovic, J. M. Baldasano, and E. Özsoy, Interactive dust-radiation modeling:
836 a step to improve weather forecasts, *J. Geophys. Res.*, 111:D16206.
837 doi:10.1029/2005JD0067172006, 2006.
- 838 Perlwitz J., R. Miller, Cloud cover increase with increasing aerosol absorptivity—a counterexample to
839 the conventional semi-direct aerosol effect, *J. Geophys. Res.*, 115:D08203.
840 doi:10.1029/2009JD012637, 2010.
- 841 Perlwitz, J. P., Pérez García-Pando, C., and R. L. Miller, Predicting the mineral composition of dust
842 aerosols – Part 1: Representing key processes, *Atmos. Chem. Phys.*, 15, 11593-11627,
843 doi:10.5194/acp-15-11593-2015, 2015a.
- 844 Perlwitz, J. P., Pérez García-Pando, C., and R. L. Miller, Predicting the mineral composition of dust
845 aerosols – Part 2: Model evaluation and identification of key processes with observations, *Atmos.*
846 *Chem. Phys.*, 15, 11629-11652, doi:10.5194/acp-15-11629-2015, 2015b.
- 847 Petzold, A., Schönlinner, M., Multi-angle absorption photometry - a new method for the measurement
848 of aerosol light absorption and atmospheric black carbon, *J. Aerosol Sci.* 35, 421-441, 2004.
- 849 Petzold, A., Rasp, K., Weinzierl, B., Esselborn, M., Hamburger, T., Dornbrack, A., Kandler, K., Schütz,
850 L., Knippertz, P., Fiebig, M., Virkkula, A., Saharan dust absorption and refractive index from
851 aircraft-based observations during SAMUM 2006, *Tellus B* 61: 118–130, 2009.
- 852 [Petzold, A., Veira, A., Mund, S., Esselborn, M., Kiemle, C., Weinzierl, B., Hamburger, T., Ehret, G.,
853 Lieke, K., and Kandler, K.: Mixing of mineral dust with urban pollution aerosol over Dakar
854 \(Senegal\): impact on dust physico-chemical and radiative properties, *Tellus*, 63B, 619-634, doi:
855 \[10.1111/j.1600-0889.2011.00547.x\]\(#\), 2011.](#)

- 856 [Petzold, A., Onasch, T., Keabian, P. and Freedman, A., Interecomparison of a Cavity Attenuated Phase](#)
857 [Shift-based extinction monitor \(CAPS PMex\) with an integrating nephelometer and a filter-based](#)
858 [absorption monitor, Atmos. Meas. Tech., 6, 1141–1151, doi:10.5194/amt-6-1141-2013, 2013.](#)
- 859 Ravel, B., and M. Newville, ATHENA, ARTEMIS, HEPHAESTUS: data analysis for X-ray absorption
860 spectroscopy using IFEFFIT, *J. Synchrotron Radiation* 12, 537–541,
861 doi:10.1107/S0909049505012719, 2005.
- 862 Ryder, C. L., Highwood, E. J., Rosenberg, P. D., Trembath, J., Brooke, J. K., Bart, M., Dean, A., Crosier,
863 J., Dorsey, J., Brindley, H., Banks, J., Marsham, J. H., McQuaid, J. B., Sodemann, H., and Wash-
864 ington, R., , Optical properties of Saharan dust aerosol and contribution from the coarse mode as
865 measured during the Fennec 2011 aircraft campaign, *Atmos. Chem. Phys.*, 13, 303-325,
866 doi:10.5194/acp-13-303-2013, 2013a.
- 867 Ryder, C. L., E. J. Highwood, T. M. Lai, H. Sodemann, and J. H. Marsham, Impact of atmospheric
868 transport on the evolution of microphysical and optical properties of Saharan dust, *Geophys. Res.*
869 *Lett.*, 40, 2433–2438, doi:10.1002/grl.50482, 2013b.
- 870 Scanza, R. A., Mahowald, N., Ghan, S., Zender, C. S., Kok, J. F., Liu, X., Zhang, Y., and Albani, S.:
871 Modeling dust as component minerals in the Community Atmosphere Model: development of
872 framework and impact on radiative forcing, *Atmos. Chem. Phys.*, 15, 537–561, doi:10.5194/acp-
873 15-537-2015, 2015.
- 874 [Sertsu, S. M., and Sánchez, P. A., Effects of Heating on Some Changes in Soil Properties in Relation to](#)
875 [an Ethiopian Land Management Practice, Soil Sci. Soc. Am. J., 42, 940–944, 1978.](#)
- 876 Shen, Z. X., J. J. Cao, R. Arimoto, R. J. Zhang, D. M. Jie, S. X. Liu, and C. S. Zhu, Chemical composition
877 and source characterization of spring aerosol over Horqin sand land in northeastern China, *J.*
878 *Geophys. Res.*, 112, D14315, doi:10.1029/2006JD007991, 2007.
- 879 Sinyuk, A., O. Torres, and O. Dubovik, Combined use of satellite and surface observations to infer the
880 imaginary part of refractive index of Saharan dust, *Geophys. Res. Lett.*, 30(2), 1081,
881 doi:10.1029/2002GL016189, 2003.
- 882 Slingo, A., et al., Observations of the impact of a major Saharan dust storm on the atmospheric radiation
883 balance, *Geophys. Res. Lett.*, 33, L24817, doi:10.1029/2006GL027869, 2006.
- 884 [Sokolik, I., and Toon, O., Incorporation of mineralogical composition into models of the radiative prop-](#)
885 [erties of mineral aerosol from UV to IR wavelengths, J. Geophys. Res., 104\(D8\), 9423–9444,](#)
886 [1999.](#)
- 887 Solmon, F., Mallet, M., Elguindi, N., Giorgi, F., Zakey, A. and Konaré, A., Dust aerosol impact on
888 regional precipitation over western Africa, mechanisms and sensitivity to absorption properties,
889 *Geophys. Res. Lett.*, 35, L24705, doi:10.1029/2008GL035900, 2008.
- 890 [Sun J., Zhang, M., and Liu, T., Spatial and temporal characteristics of dust storms in China and its](#)
891 [surrounding regions, 1960–1999: Relations to source area and climate, J. Geophys. Res.,](#)
892 [106\(D10\), 10325–10333, 2001.](#)
- 893 [Sun, Y., G. Zhuang, Y. Wang, X. Zhao, J. Li, Z. Wang, and Z. An \(2005\), Chemical composition of dust](#)
894 [storms in Beijing and implications for the mixing of mineral aerosol with pollution aerosol on the](#)
895 [pathway, J. Geophys. Res., 110, D24209, doi:10.1029/2005JD006054.](#)

896 Tegen, I., and Lacis, A. A., Modeling of particle size distribution and its influence on the radiative prop-
897 erties of mineral dust aerosol, *J. Geophys. Res.*, doi:10.1029/95JD03610, 1996.

898 Torres, O., A. Tanskanen, B. Veihelmann, C. Ahn, R. Braak, P. K. Bhartia, P. Veefkind, and P. Levelt,
899 Aerosols and surface UV products from Ozone Monitoring Instrument observations: An over-
900 view, *J. Geophys. Res.*, 112, *D24S47*, doi:10.1029/2007JD008809, 2007.

901 ~~Utry, N., Ajtai, T., Filep, Á., Pintér, M., Hoffer, A., Bozóki, Z., and Szabó, G., Mass specific optical~~
902 ~~absorption coefficient of HULIS aerosol measured by a four-wavelength photoacoustic spec-~~
903 ~~trometer at NIR, VIS and UV wavelengths, *Atmos. Environ.* 69, 321–324, 2013.~~

904 Utry, N., Ajtai, T., Filep, Á., Pintér, M., Tombacz, E., Bozóki, Z., and Szabó, G., Correlations between
905 absorption Ångström exponent (AAE) of wintertime ambient urban aerosol and its physical and
906 chemical properties, *Atmos. Environ.* 91, 52–59, 2014.

907 Xian, P., Seasonal migration of the ITCZ and implications for aerosol radiative impact. PhD thesis,
908 Columbia University, 2008.

909 Vinoj, V., Rasch, P. J., Wang, H., Yoon, J.-H., Ma, P.-L., Landu, K., and Singh, B., Short-term modu-
910 lation of Indian summer monsoon rainfall by West Asian dust, *Nat. Geosci.*, 7, 308–313,
911 doi:10.1038/ngeo2107, 2014.

912 Wang, J., J. F. Doussin, S. Perrier, E. Perraudin, Y. Katrib, E. Pangui, and B. Picquet-Varrault, Design
913 of a new multi-phase experimental simulation chamber for atmospheric photosimulation, aerosol
914 and cloud chemistry research, *Atmos. Meas. Tech.*, 4, 2465–2494, 2011.

915 Wang, L., Z. Li, Q. Tian, Y. Ma, F. Zhang, Y. Zhang, D. Li, K. Li, and L. Li, Estimate of aerosol
916 absorbing components of black carbon, brown carbon, and dust from ground-based remote sens-
917 ing data of sun-sky radiometers, *J. Geophys. Res. Atmos.*, 118, 6534–6543,
918 doi:10.1002/jgrd.50356, [20132016](https://doi.org/10.1002/jgrd.50356).

919 Weinzierl, B., et al., , Microphysical and optical properties of dust and tropical biomass burning aerosol
920 layers in the Cape Verde region—an overview of the airborne in situ and lidar measurements
921 during SAMUM-2, *Tellus B*, 63(4), 589–618, 2011.

922 Yang, M., Howell, S.G., Zhuang, J., Huebert, B.J., Attribution of aerosol light absorption to black car-
923 bon, brown carbon, and dust in China - interpretations of atmospheric measurements during
924 EAST-AIRE, *Atmos. Chem. Phys.* 9, 2035e2050, 2009.

925 Zhang, X. Y., Y. Q. Wang, X. C. Zhang, W. Guo, T. Niu, S. L. Gong, Y. Yin, P. Zhao, J. L. Jin, and M.
926 Yu, Aerosol monitoring at multiple locations in China: contributions of EC and dust to aerosol
927 light absorption, *Tellus B*, 60(4), 647–656, 2008.

928 Zhao, C., Liu, X., Ruby Leung, L., and Hagos, S.: Radiative impact of mineral dust on monsoon precip-
929 itation variability over West Africa, *Atmos. Chem. Phys.*, 11, 1879–1893, 10.5194/acp-11-1879-
930 2011, 2011.

931

932 **Table captions**

933 **Table 1.** Characteristics of the standards used for the quantification of the iron oxides in the XAS anal-
934 ysis.

935 **Table 2.** ~~Summary-Geographical~~ of information on the soil samples used in this work.

936 **Table 3.** Chemical characterisation of the dust aerosols in PM_{10.6} and PM_{2.5} (in parentheses) size frac-
937 tions. Columns 3 and 4 ~~report-give~~ the Si/Al and Fe/Ca elemental ratios obtained from X-Ray Fluores-
938 cence analysis. The uncertainty of ~~fa~~ each individual value is estimated to be 10%. Column 5 ~~reports~~
939 ~~shows~~ $MR_{Fe\%}$, the fractional mass of elemental iron with respect to the total dust mass concentration
940 (uncertainty 10%). Column 5 reports $MR_{Fe\%}$, the mass fraction of iron oxides with respect to the total
941 dust mass concentration (uncertainty 15%). For PM_{2.5} the determination of the Si/Al ratio is impossible
942 due to the composition of the filter ~~medium-membranes~~ (quartz).

943 **Table 4.** Mass absorption efficiency (MAE, $10^{-3} \text{ m}^2 \text{ g}^{-1}$) and Ångström Absorption Exponent (AAE) in
944 the PM_{10.6} and PM_{2.5} size fractions. Absolute errors are in brackets.

945 **Table 5.** Mass absorption efficiency (MAE, $10^{-3} \text{ m}^2 \text{ g}^{-1}$) and Ångström Absorption Exponent (AAE) ~~of~~
946 ~~from the~~ literature data discussed in the paper

947

948 **Figure captions**

949 **Figure 1.** Time series of aerosol mass concentration in the chamber for ~~the~~ two companion experiments
950 (Libyan ~~dust-sample~~). Experiment 1 (top panel) was dedicated to the determination of the chemical
951 composition (including iron oxides) by sampling on polycarbonate filters. Experiment 2 (bottom panel)
952 was dedicated to the determination of the absorption optical properties by sampling on quartz filters.

953 **Figure 2.** Locations (red stars) of the soil and sediment samples used to generate dust aerosols.

954 **Figure 3.** Spectral dependence of the MAE values for the samples investigated in this study in the PM_{10.6}
955 (left) and in the PM_{2.5} (right) mass fractions.

956 **Figure 4.** Illustration of the links between the MAE values and the dust chemical composition found in
957 this study. Left column, from top to bottom: linear regression between ~~the~~ MAE values ~~between-in the~~
958 ~~range from~~ 375 ~~toand~~ 850 nm and the fraction of elemental iron ~~with-respect-to-relative to~~ the total dust
959 mass ($MR_{Fe\%}$) in the PM_{10.6} fraction; Middle column: same as left column but ~~respect-tofor~~ the mass

960 fraction of iron oxides [relative](#) to the total dust mass ($MR_{Fe\ ox\%}$) in the PM_{10.6} size fraction; Right column:
961 same as left column but in the PM_{2.5} size fraction.
962

963 **Table 1.** Characteristics of the standards used for the quantification of the iron oxides in the XAS anal-
 964 ysis.

Standard	Stoechiometric Stoichiometric Formula	Origin
Illite of Puy	$(\text{Si}_{3.55}\text{Al}_{0.45})(\text{Al}_{1.27}\text{Fe}_{0.36}\text{Mg}_{0.44})\text{O}_{10}(\text{OH})_2(\text{Ca}_{0.01}\text{Na}_{0.01}\text{K}_{0.53}\text{X}(\text{I})_{0.12})$	Puy, France
Goethite	$\text{FeO} \cdot \text{OH}$	Minnesota
Hematite	Fe_2O_3	Niger
Montmorillonite	$(\text{Na},\text{Ca})_{0.3}(\text{Al},\text{Mg})_2\text{Si}_4\text{O}_{10}(\text{OH})_2 \cdot n(\text{H}_2\text{O})$	Wyoming
Nontronite	$\text{Na}_{0.3}\text{Fe}_2(\text{Si},\text{Al})_4\text{O}_{10}(\text{OH})_2 \cdot n\text{H}_2\text{O}$	Pennsylvania

965

966

967

968 **Table 2.** Geographical information on the soil samples used in this work.

Geographical area	Sample	Desert area	Geographical coordinates
Sahara	Morocco	East of Ksar Sahli	31.97°N, 3.28°W
	Libya	Sebha	27.01°N, 14.50°E
	Algeria	Ti-n-Tekraouit	23.95°N, 5.47°E
Sahel	Mali	Dar el Beida	17.62°N, 4.29°W
	Bodélé	Bodélé depression	17.23°N, 19.03°E
Middle East	Saudi Arabia	Nefud	27.49°N, 41.98°E
	Kuwait	Kuwaiti	29.42°N, 47.69°E
Southern Africa	Namibia	Namib	21.24°S, 14.99°E
Eastern Asia	China	Gobi	39.43°N, 105.67°E
North America	Arizona	Sonoran	33.15 °N, 112.08°W
South America	Patagonia	Patagonia	50.26°S, 71.50°W
Australia	Australia	Strzelecki	31.33°S, 140.33°E

969

970

971 **Table 3.** Chemical characterisation of the dust aerosols in PM_{10.6} and PM_{2.5} (in parentheses) size frac-
 972 tions. Columns 3 and 4 give the Si/Al and Fe/Ca elemental ratios obtained from X-Ray Fluorescence
 973 analysis. The uncertainty of each individual value is estimated to be 10%. Column 5 shows $MR_{Fe\%}$, the
 974 fractional mass of elemental iron with respect to the total dust mass concentration (uncertainty 10%).
 975 Column 5 reports $MR_{Fe-ox\%}$, the mass fraction of iron oxides with respect to the total dust mass concentra-
 976 tion (uncertainty 15%). For PM_{2.5} the determination of the Si/Al ratio is impossible due to the composi-
 977 tion of the filter- membranes (quartz)
 978 Chemical characterisation of the dust aerosols in PM_{10.6} and PM_{2.5} (in parentheses) size fractions. Col-
 979 umns 3 and 4 report the Si/Al and Fe/Ca elemental ratios obtained from X-Ray Fluorescence analysis.
 980 The uncertainty on each individual value is estimated to be 10%. Column 5 reports $MR_{Fe\%}$, the fractional
 981 mass of elemental iron with respect to the total dust mass concentration (uncertainty 10%). Column 5
 982 reports $MR_{Fe-ox\%}$, the mass fraction of iron oxides with respect to the total dust mass concentration (un-
 983 certainty 15%). For PM_{2.5} the determination of the Si/Al ratio is impossible due to the composition of
 984 the filter medium.
 985

Geographical area	Sample	Si/Al	Fe/Ca	MC _{Fe%}	MC _{Fe-ox%}
Sahara	Morocco	3.12 (---)	0.24 (0.28)	3.6 (4.4)	1.4 (1.8)
	Libya	2.11 (---)	1.19 (1.12)	5.2 (5.6)	3.1 (3.4)
	Algeria	2.51 (---)	3.14 (4.19)	6.6 (5.4)	2.7 (2.2)
Sahel	Mali	3.03 (---)	2.99 (3.67)	6.6 (33.6)	3.7 (18.7)
	Bodélé	5.65 (---)	12.35 (----)	4.1 (----)	0.7 (----)
Middle East	Saudi Arabia	2.95 (---)	0.29 (0.27)	3.8 (5.1)	2.6 (3.5)
	Kuwait	3.15 (---)	0.89 (1.0)	5.0 (13.6)	1.5 (4.2)
Southern Africa	Namibia	3.41 (---)	0.11 (0.10)	2.4 (6.9)	1.1 (3.1)
Eastern Asia	China	2.68 (---)	0.77 (0.71)	5.8 (13.6)	0.9 (2.5)
North America	Arizona	3.30 (---)	0.95 (----)	5.3 (----)	1.5 (----)
South America	Patagonia	4.80 (---)	4.68 (4.64)	5.1 (----)	1.5 (---)
Australia	Australia	2.65 (---)	5.46 (4.86)	7.2 (11.8)	3.6 (5.9)

986

987

988 **Table 4.** Mass absorption efficiency (MAE, $10^{-3} \text{ m}^2 \text{ g}^{-1}$) and Ångström Absorption Exponent (AAE) in
 989 the $\text{PM}_{10.6}$ and $\text{PM}_{2.5}$ size fractions. Absolute errors are in brackets.

		PM_{10.6}					
Geographical area	Sample	375 nm	407 nm	532 nm	635 nm	850 nm	AAE
Sahara	Morocco	--- (---)	--- (---)	--- (---)	--- (---)	--- (---)	--- (---)
	Libya	89 (11)	75 (9)	30 (5)	--- (---)	--- (---)	3.2 (0.3)
	Algeria	99 (10)	80 (10)	46 (7)	16 (3)	15 (3)	2.5 (0.3)
Sahel	Mali	--- (---)	103 (18)	46 (12)	--- (---)	--- (---)	--- (---)
	Bodélé	37 (4)	25 (3)	13 (2)	6 (1)	3 (1)	3.3 (0.3)
Middle East	Saudi Arabia	90 (9)	79 (8)	28 (3)	6 (1)	4 (1)	4.1 (0.4)
	Kuwait	--- (---)	--- (---)	--- (---)	--- (---)	--- (---)	2.8 (0.3)
Southern Africa	Namibia	52 (7)	49 (7)	13 (3)	5 (2)	1 (2)	4.7 (0.5)
Eastern Asia	China	65 (8)	58 (7)	32 (4)	8 (2)	7 (2)	3 (0.3)
North America	Arizona	130 (15)	99 (12)	47 (7)	21 (4)	13 (4)	3.1 (0.3)
South America	Patagonia	102 (11)	80 (9)	29 (4)	17 (2)	10 (2)	2.9 (0.3)
Australia	Australia	135 (15)	121 (13)	55 (7)	26 (4)	14 (3)	2.9 (0.3)

990
991

PM _{2.5}							
Geographical area	Sample	375 nm	407 nm	532 nm	635 nm	850 nm	AAE
Sahara	Morocco	107 (13)	88 (11)	34 (6)	14 (3)	15 (4)	2.6 (0.3)
	Libya	132(17)	103 (14)	33 (7)	--- (---)	--- (---)	4.1 (0.4)
	Algeria	95(8)	71 (11)	37 (7)	12 (5)	12 (5)	2.8 (0.3)
Sahel	Mali	711 (141)	621 (124)	227 (78)	--- (---)	--- (---)	3.4 (0.3)
	Bodelé	--- (---)	--- (---)	--- (---)	--- (---)	--- (---)	--- (---)
Middle East	Saudi Arabia	153 (18)	127 (15)	42 (7)	8 (4)	6 (4)	4.5 (0.5)
	Kuwait	270 (100)	324 (96)	--- (---)	54 (52)	--- (---)	3.4 (0.3)
Southern Africa	Namibia	147 (36)	131 (32)	31 (21)	6 (16)	3 (15)	5.1 (0.5)
Eastern Asia	China	201 (30)	176 (26)	89 (17)	14 (10)	23 (10)	3.2 (0.3)
North America	Arizona	--- (---)	--- (---)	--- (---)	--- (---)	--- (---)	--- (---)
South America	Patagonia	--- (---)	--- (---)	--- (---)	--- (---)	--- (---)	2.9 (0.3)
Australia	Australia	335 (39)	288 (33)	130 (19)	57 (11)	36 (9)	2.9 (0.3)

992
993

994 **Table 5.** Mass absorption efficiency (MAE, $10^{-3} \text{ m}^2 \text{ g}^{-1}$) and Ångström Absorption Exponent (AAE)
 995 [from the efliterature data](#) discussed in the paper

Geo- graphical area	Sample	266 nm	325 nm	428 nm	532 nm	660 nm	880 nm	106 4 nm	AAE
	Morocco*								2.25– 5.13
	Morocco, PM _{2.5} [‡]								2.0–6.5
Sa- hara	Morocco, submicron [#]	1100			60			30	4.2
	Egypt, submicron [#]	810			20				5.3
	Tunisia [§]		83			11			
	Saharan, transported ^μ								2.9 ± 0.2
	Saharan, transported (PM ₁₀) [¶]			37	27 ^{%%}	15 ^{%%%}			2.9
	Saharan, transported (PM ₁) [¶]			60	40 ^{%%}	30 ^{%%%}			2.0
Sahel	Niger [§]		124			19			
East- ern Asia	China [§]		69			10			
	China ^{&}		87 ^{&}	50 ^{&&&}	27 ^{&&&}	13	1		3.8
Ara- bian Penin- sula, N/NE Af- rica, Cen- tral Asia	Various locations [@]								2.5-3.9

996 * Müller et al. (2008)

997 ‡ Petzold et al. (~~2008~~2009)

998 # Linke et al. (2006)

999 § Alfaro et al. (2004)

1000 ^μ Fialho et al. (2005)

1001 [¶] Denjean et al. (2016); ^{%%} at 528 nm, ^{%%%} at 652 nm

1002 [&] Yang et al. (2009); ^{&&} at 375 nm, ^{&&&} at 470 nm, ^{&&&&} at 590 nm

1003 [@] Mossmüller et al. (2012)

1004

1005

1006

1007

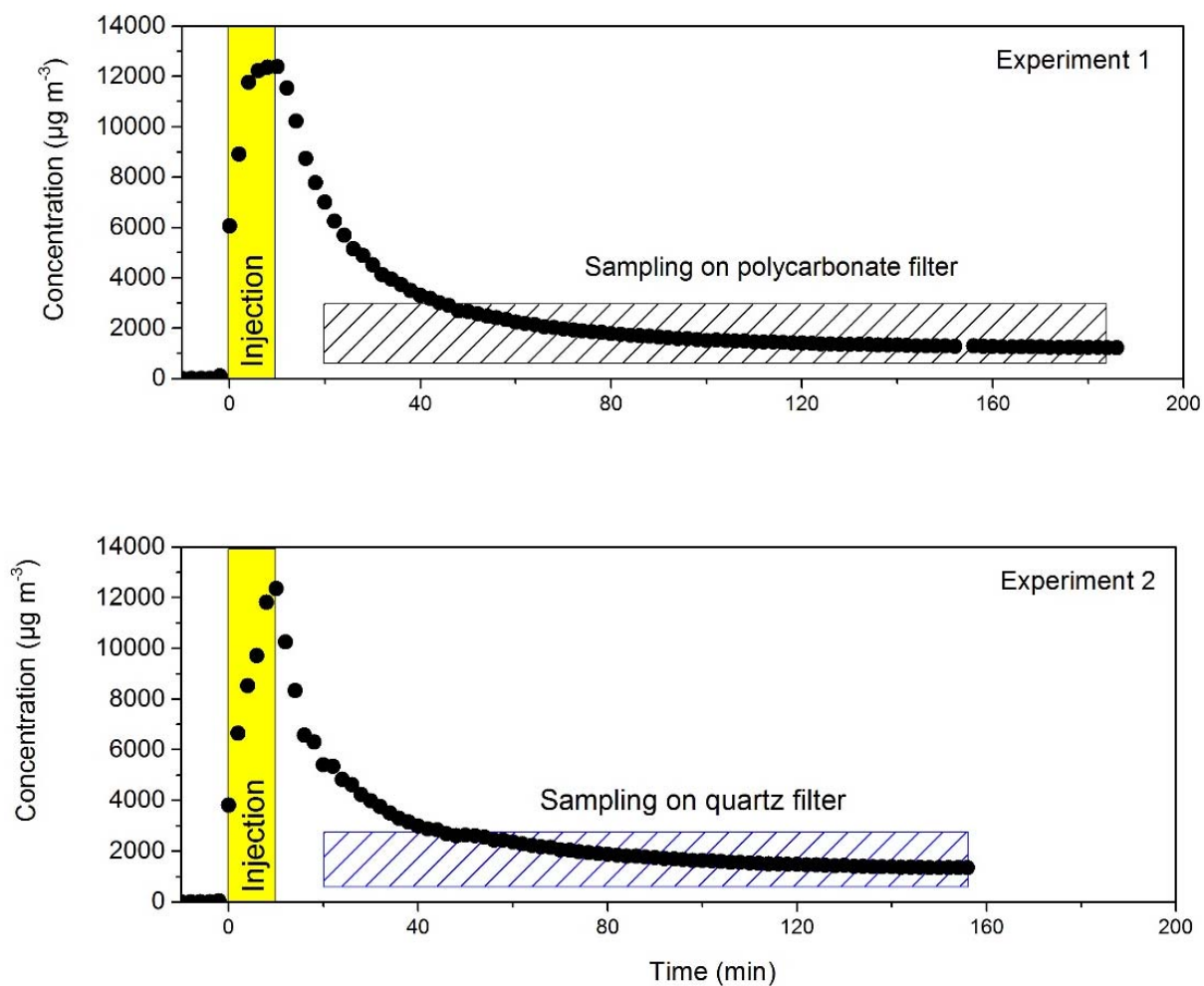
1008

1009

1010

1011

Figure 1. [Time series of aerosol mass concentration in the chamber for two companion experiments \(Libyan dust\).](#) ~~Time series of aerosol mass concentration in the chamber for the two companion experiments (Libya sample).~~ Experiment 1 (top panel) was dedicated to the determination of the chemical composition (including iron oxides) by sampling on polycarbonate filters. Experiment 2 (bottom panel) was dedicated to the determination of the absorption optical properties by sampling on quartz filters.

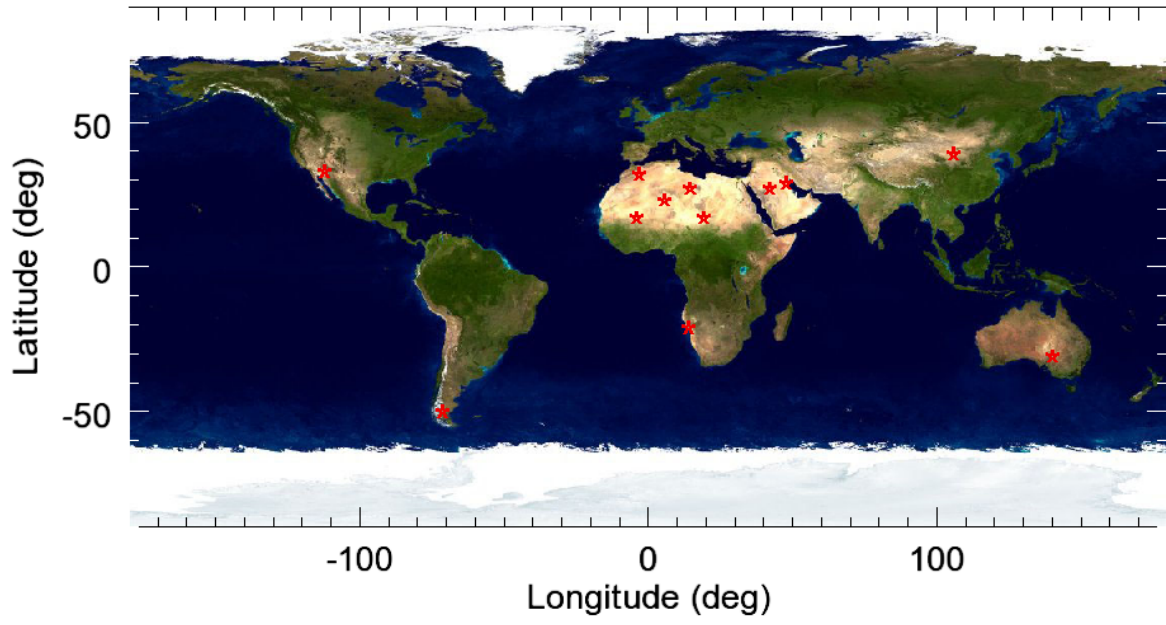


1012

1013

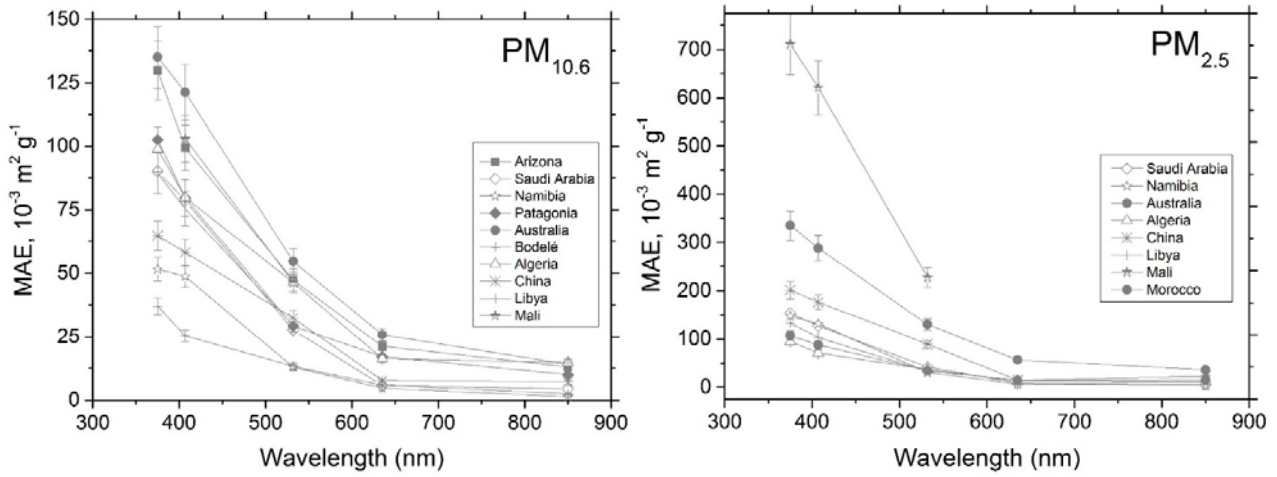
1014

1015 **Figure 2.** Locations (red stars) of the soil and sediment samples used to generate dust aerosols.



1016
1017

1018 **Figure 3.** Spectral dependence of the MAE values for the samples investigated in this study in the PM_{10.6}
1019 (left) and in the PM_{2.5} (right) mass fractions.

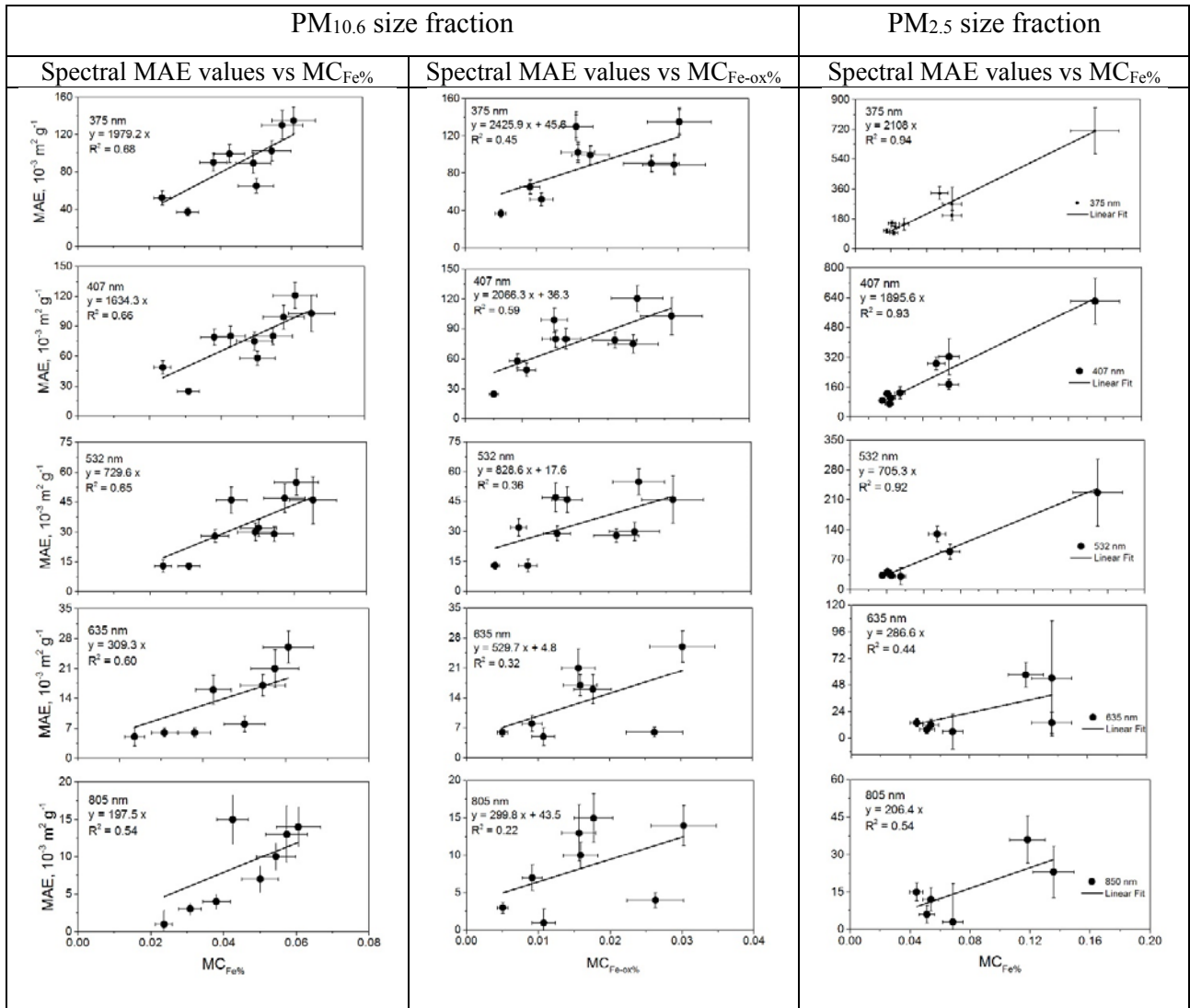


1020

1021 **Figure 4.** Illustration of the links between the MAE values and the dust chemical composition found in
1022 this study. Left column, from top to bottom: linear regression between the MAE values in the range from
1023 375 to 850 nm and the fraction of elemental iron relative to the total dust mass ($MR_{Fe\%}$) in the $PM_{10.6}$
1024 fraction; Middle column: same as left column but for the mass fraction of iron oxides relative to the total
1025 dust mass ($MR_{Fe\ ox\%}$) in the $PM_{10.6}$ size fraction; Right column: same as left column but in the $PM_{2.5}$ size
1026 fraction.

1027 ~~Illustration of the links between the MAE values and the dust chemical composition found in this study.~~
1028 ~~Left column, from top to bottom: MAE values between 375 and 850 nm versus the fraction of elemental~~
1029 ~~iron with respect to the total dust mass ($MR_{Fe\%}$) in the $PM_{10.6}$ fraction; Middle column: same as left~~
1030 ~~column but versus the mass fraction of iron oxides to the total dust mass ($MR_{Fe\ ox\%}$) in the $PM_{10.6}$ size~~
1031 ~~fraction; Right column: same as left column but in the $PM_{2.5}$ size fraction. The linear regression lines~~
1032 ~~between MAE and $MR_{Fe\%}$ and MAE and $MR_{Fe\ ox\%}$ are reported in each plot.~~

1033
1034
1035
1036
1037
1038
1039
1040
1041
1042
1043
1044
1045
1046
1047
1048
1049
1050
1051



1052
1053